Russian Chemical Reviews **77** (1) 21 – 37 (2008) © 2008 Russian Academy of Sciences and Turpion Ltd

DOI 10.1070/RC2008v077n01ABEH003748

Exothermic reaction waves in multilayer nanofilms

A S Rogachev

Contents

I.	Introduction	21
II.	Methods for preparation and structures of reactive multilayer nanofilms	22
III.	Reaction wave propagation in nanofilms	24
IV.	Mathematical models for reaction wave propagation in nanofilms	28
V.	Dynamics of phase and structural transformations in heterogeneous reactions in nanoscale systems	31
VI.	Practical application	35
VII.	Conclusion	35

Abstract. Experimental and theoretical studies on heterogeneous exothermic reaction waves in multilayer nanofilms are analysed. Mathematical models for the reaction wave propagation are described. The dynamics of phase and structural transformations during heterogeneous reactions in nanoscale systems is considered. Prospects of the studies of reaction waves for the elucidation of the mechanisms of processes in nanoscale systems and for diverse practical applications (in particular, for the development of new welding and soldering techniques) are demonstrated. The bibliography includes 113 references.

I. Introduction

The discovery of the self-propagating high-temperature synthesis (SHS) made 40 years ago [1, 2] gave rise to the development of many new research and technological fields in chemistry, chemical physics and materials science. One of areas of investigation that emerged in the mid-1990s is associated with research on self-sustaining reaction waves in thin films consisting of hundreds or thousands of alternating layers of the reactants, the thickness of each layer varying from several nanometers to micrometers. Attempts to perform the SHS process in layered systems (for example, in foil rolls) have been made earlier.[3, 4] However, the design of nanostructured multilayer systems in which the exothermic reaction self-propagates (without external heating) due to heat release became possible only with the development of methods of deposition of very thin alternating layers. A publication [5] describing a self-sustaining reaction in a multilayer nickel – aluminium nanofilm (with a total thickness of 300 nm) separated from an inert support for the first time is a pioneering study in this field.

A patent [6] that simultaneously covers a method for the preparation of nanostructured multilayer films and wave reactions in these films played an exceptionally important role in the progress in this field of investigation. In the last decade, the number of scientific publications dealing with investigations and practical applications of these films steadily increased. Since this area of investigation is at the interface of chemical physics of combustion and explosion processes, chemistry and materials science, the results of studies are published in journals of different disciplines. Abundant data were published in physical journals; other, in materials science journals. However, since chemical reactions provide the basis of the processes under consideration, these materials are of interest for chemists as well.

The aim of the present review was to summarise and critically analyse the results of studies in this field published in the last decade and reveal the trends of research. The present review considers only exothermic multilayer systems, which can react in the self-sustaining mode (the combustion wave or thermal explosion). Numerous other reactions in thin films, including those in nanolayers that are not accompanied by heat release sufficient for the self-sustaining mode are beyond the scope of the present review. The interested reader can go to numerous publications (including the monograph [7]) where these reactions were considered. At the same time, results of experimental studies in which films were subjected to relatively slow heating and investigated by such methods as differential scanning calorimetry (DSC) or time-resolved X-ray diffraction using synchrotron radiation (TRXRD-SR) are of great importance for understanding of the mechanisms and steps of reactions. The experimental studies are considered in the context of their significance for the analysis of self-sustaining reactions.

A S Rogachev Institute of Structural Macrokinetics and Materials Science, Russian Academy of Sciences, ul. Institutskaya 8, 142432 Chernogolovka, Moscow Region, Russian Federation. Fax (7-495) 962 80 25, tel. (7-495) 962 80 34, e-mail: rogachev@ism.ac.ru

Received 20 August 2007
Uspekhi Khimii **77** (1) 22 – 38 (2008); translated by T N Safonova

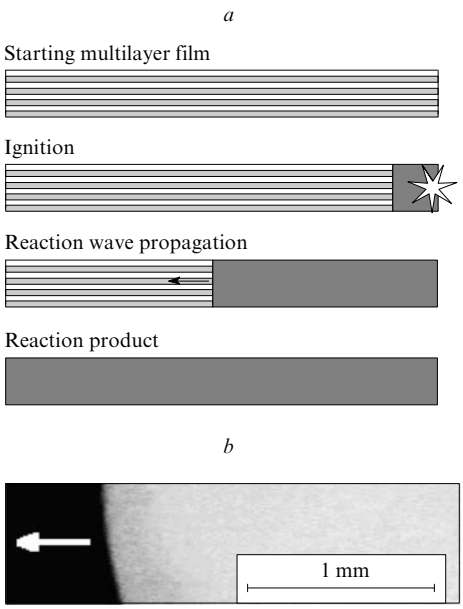


Figure 1. Scheme of the reaction wave in a nanofilm (*a*) and a video image of the reaction wave[8] in the Ti/3Al film (*b*).

The reaction in a multilayer Ti/3Al nanofilm † is schematically presented in Fig. 1. The figure also shows a video image of the glowing reaction wave.[8] Reaction waves in nanofilms are characterised by unusually high (up to tens of metres per second!) propagation rates and the abnormally low temperature of initiation of the solid-state reaction (400 – 600 K). These parameters do not fit in the context of the kinetics of heterogeneous solid-state reactions, diffusion processes and mechanisms of solid-flame combustion. This review presents the critical analysis of studies providing a new theoretical basis for the observed phenomena.

In spite of the fact that reactive nanofilms have attracted the attention of researchers rather recently, they have already found commercial use. Practical problems solved with the use of reactive nanofilms and possible fields of their application in the nearest future are also considered.

II. Methods for preparation and structures of reactive multilayer nanofilms

1. Layer-by-layer magnetron sputtering

Homogeneous layers can be deposited by the magnetron sputtering during a long period of time at a constant layer growth rate. This is of great importance for the deposition of a huge number (hundreds and thousands) of alternating layers.

† According to the classification that has been developed in this field of investigation, by reactive nanofilms let us mean films consisting of different nanoscale thickness layers capable of being involved in exothermic reactions (in spite of the fact that the total film thickness can be as large as tens of micrometers). The chemical composition of samples will be described using the following conventional notations: the 'A – B system' refers to all films containing layers of components (reactants) A and B regardless of their quantitative ratio; the 'film A/B' signifies that the ratio between the compounds A and B in two adjacent layers corresponds to the equimolar average composition of the film (correspondingly, A/3B refers to two adjacent layers of the film containing one mole of the component A per three moles of the component B, *etc.*).

In essence, the method of deposition of reactive multilayer nanofilms[6,9] is analogous to the method of deposition of multilayer coatings developed earlier.[10,11] The scheme of the method is presented in Fig. 2. The reactants are sputtered from two (or more) simultaneously operating sources (magnetron targets). The substrates are fixed on a rotating holder and alternately exposed to a flow of the substance that is deposited from different targets. The number of layers is equal to the number of revolutions of the holder, and the thickness of each layer is determined by the exposure time (the rotation speed), the power of the source and the source-to-substrate distance.

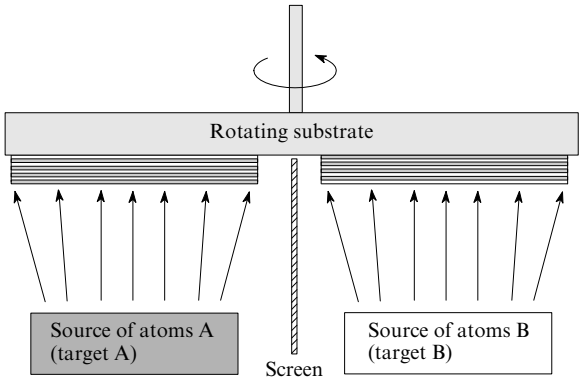


Figure 2. Scheme illustrating the procedure for the preparation of multilayer films by sputtering.

Generally, the process is carried out in special-purity rarefied argon at a pressure of up to tens of Pascal (the sputter chamber is preevacuated to high vacuum). It is necessary to maintain low temperature of the substrate to avoid the reaction between the layers and suppress the mutual diffusion in the deposition step. Generally, the temperature of the substrate is close to room temperature throughout the deposition of the film. The microstructure of the reactive film consisting of layers of different thickness is shown in Fig. 3. It can be seen that the layers remain planar and do not lose the continuity as their thickness decreases.

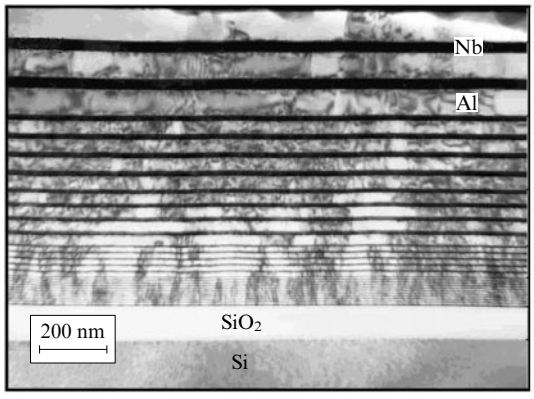


Figure 3. Cross-section of the Nb/Al film consisting of variable thickness layers deposited on a silicon substrate coated with a silicon oxide layer.[12] The image was obtained with a transmission electron microscope.

Reactive multilayer systems have an excess of chemical energy, energy of elastic stresses of layers and free energy of

interfaces.[13] This excess creates the thermodynamic driving force, which can destroy the layers and lead to their mixing or breaking (the formation of islands instead of continuous layers). In addition, each layer is polycrystalline, *i.e.*, consists of a mosaic of planar grains with interfaces located perpendicular to the interface between the layers. An analysis of stability of multilayer films taking into account the excess energy of interfaces showed[13] that the layers are more planar if the specific (per unit surface area) energy of interfaces between the grains is substantially lower than the specific energy of interfaces between the layers. In the case of the inverse ratio, characteristic grooves appear at the intersection of grain and layer interfaces; these grooves can lead to breaking of the layers.

The surface roughness due to grain interfaces is clearly seen in a photomicrograph of the film surface obtained with a scanning tunneling microscope (Fig. 4 *a*). Due to the energy excess at the grain interfaces, the centre of the grain grows more rapidly than its periphery, resulting in the dome-shaped surface of the grains. The dome height is, on the average, 5–10 nm; the grain diameter is $\sim$500 nm (Fig. 4 *b*). The layer roughness varies depending on the composition of the system, the layer thickness, the properties of the substrate and other parameters. It is unlikely that it is possible to accurately predict the microstructure of layers, and consequently, it is necessary to determine the microstructure by experimental methods for each particular system.

Multilayer films prepared by the magnetron sputtering method are characterised by the presence of a texture. The texture manifests itself in the fact that predominantly the same atomic planes are oriented along the layers in the crystal structure of different grains composing polycrystalline films. This phenomenon is well known from the practice of the preparation of thin films.[7]

Therefore, in spite of the seemingly simple structure of multilayer films, they have a complex microstructure and, taking into account the layer size, a complex nanostructure. There are the following important characteristics of nanostructures reported in almost all studies performed in this field: the period, *i.e.*, the total thickness of two adjacent layers (d),‡ and the total film thickness (H). The influence of this nanostructure on the reaction mechanism is discussed below.

The reactive films in the systems Ni–Al,[15,16] Ti–Al,[15,16] Ti–Al,[8,14,17–22] Nb–Al,[12,23,24] Ta–Al,[24] Cu–Al,[24] Nb–Si,[6,25] CuO–Al,[26,27] *etc.* were synthesised by the magnetron sputtering method and studied. It can be stated that this is the main method in the synthesis of nanofilms used for studying self-sustaining reactions in these films. Other methods of deposition (such as chemical gas-phase deposition or galvanic methods) have not found use in this field due apparently to technical difficulties of the formation of a large number of alternating layers. Films consisting of alternating continuous layers with thickness larger than 3–4 nm were synthesised by the magnetron sputtering method; the number of layers in films can be larger than 5000.[21]

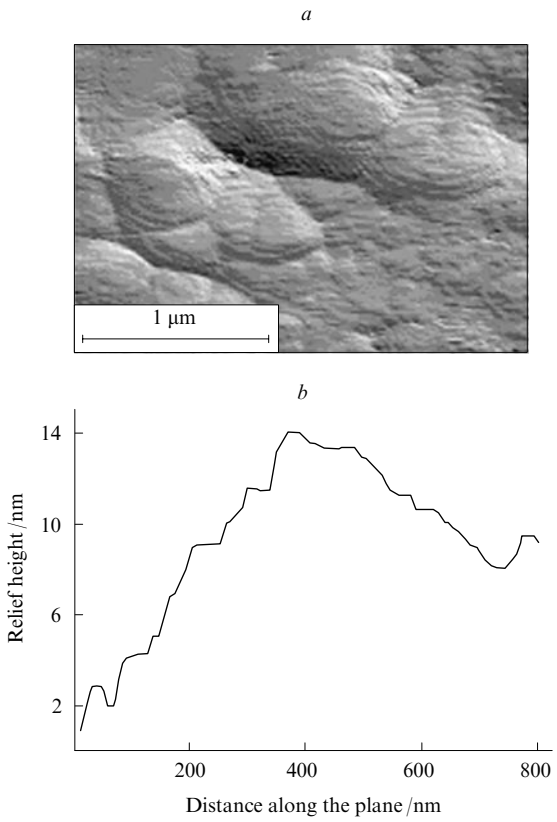


Figure 4. Photomicrograph of the surface (*a*) and the surface profile (*b*) of the Ti/Al film (the layer thickness is 60 nm).[14]
The image was obtained with a scanning tunneling microscope.

2. Vacuum deposition

The high-vacuum vapour deposition allows the preparation of very thin (up to several Ångströms) layers of specified composition. However, it is difficult to achieve a constant rate of evaporation during a long period of time necessary for deposition of hundreds or thousands of layers. Hence, this method has found use only for the synthesis of films consisting of a relatively small number of layers. The reaction wave propagation in two-layer Al/Ni, Al/Fe and Al/Co films consisting of layers with thickness of 30–100 nm (the thickness of the film was no larger than 200 nm) was studied.[28,29] Layers were deposited by evaporation–deposition *in vacuo* (10^{-4} Pa). In the early study[5] on combustion of multilayer (up to several tens of layers) films belonging to the Ni–Al system, the films were synthesised by vacuum electron-beam evaporation (10^{-6} Pa); the total film thickness is generally 300 nm. Multilayer films of the Pt–Co system[30] containing from 60 to 90 pairs of layers were synthesised by the vacuum deposition method; the thickness of the cobalt layer was 0.40–0.44 nm and the thickness of the platinum layer was 0.51–0.55 nm. The high-vacuum electron-beam evaporation (10^{-6} Pa) was used also for the preparation of the reactive multilayer films of the Ti–Si system[31] consisting of titanium layers with thickness of 14–18 nm and silicon layers with thickness of 16–42 nm; the number of the layers is generally equal to 10 (5 layers of each reactant). The layers deposited *in vacuo* often have an amorphous atomic structure.

3. Mechanical methods for preparation of reactive multilayer films

Low efficiency and high cost of vacuum deposition and magnetron sputtering methods are their main drawbacks.

‡ The period of the multilayer structure is sometimes called the bilayer thickness. This value is equal to the sum of the thicknesses of two adjacent layers of different reactants (for example, the thickness of one Ni layer + the thickness of one Al layer).

Hence, more efficient and cheaper methods for the preparation of multilayer nanofilms are being actively developed. Among these methods, the multiple rolling is of most interest. For example, films with a double layer thickness of 2.6 nm and the total number of layers >5000 were prepared in the Ag—Ni system by the following method.[32] Thin silver (9 μm) and nickel (14 μm) foils were packed in an alternating order (250 foils), pressed and annealed at 1073 K for one hour. The resulting multilayer sample was rolled to a thickness of 0.2 mm. Then 21 rolled samples were packed in a stack and subjected to hot pressing and rolling. In some cases, the procedure was repeated. It was concluded that this method can be used for preparing layered nanocomposites.[32]

A similar method was applied to the preparation of reactive multilayer films in the Ni—Al system,[33] up to 70 cycles of rolling being used. This process afforded a film consisting of nickel and aluminium layers with thickness of <100 nm (Fig. 5 *a*). A more regular layered nanostructure was prepared by rolling platinum and aluminium foils (Fig. 5 *b*).[34] As can be seen from the figures, at a higher degree of thinning of the foils in the course of rolling, many layers become wavy and breaking of less plastic layers often occurs.

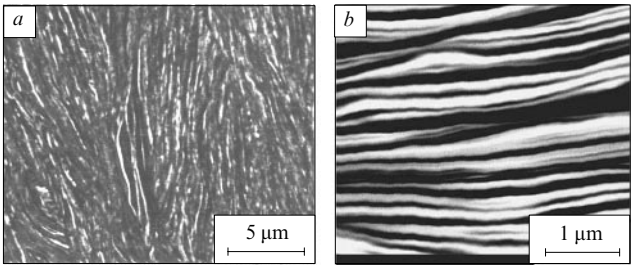


Figure 5. Microstructures of multilayer films prepared from alternating foils.
(*a*) Nickel layers (pale) and aluminum layers (dark) after 70 cycles of soldering ;[33] (*b*) platinum layers (pale) and aluminium layers (dark).[34] The images were obtained with a scanning reflection electron microscope.

The simultaneous rolling of metal foils having substantially different mechanical properties (the yield stress, the modulus of elasticity, the Poisson coefficient) is a complex and sometimes insoluble problem. To overcome these difficulties, one can use composite multilayer species prepared by the mechanical activation [35, 36] for rolling. A mixture of powdered reagents was extensively treated in planetary ball mills,[37, 38] which was accompanied by sticking and manifold flattening of the particles of plastic components (reactants) and grinding of fragile components (reactants) under the action of high-speed collisions of milling balls. This allows the preparation of multilayer composite particles with a layer thickness of 100–200 nm and smaller. It is easier to synthesise multilayer nanofilms by the cold rolling from such particles rather than from foils or particles of individual reactants.

An interesting approach applied in the study [39] also deserves notice. In this study, multilayer nanofilms of the Nb–Al system were prepared by the magnetron deposition followed by the rolling. The aim of the investigation was to study the mechanical properties of multilayer nanofilms. However, it is not inconceivable that this 'hybrid' method can be efficient in the production of particular types of films.

The review of the methods for preparation of multilayer nanofilms showed that there is a considerable scope for studies in this area. On the one hand, it is necessary to increase the efficiency and decrease the cost of magnetron and vacuum deposition methods. On the other hand, it is necessary to improve mechanical methods to prepare films with more regular and perfect structures. As follows from the analysis of the published data, the chemical and electrochemical deposition methods have not yet attracted the attention of researchers engaged in the synthesis of multilayer nanofilms, although the electrodeposition of nanocomposites with a grain structure has been studied.[40–42] In our opinion, a combination of the layer-by-layer chemical (electrochemical) deposition and the subsequent rolling offers promise. Apparently, the rapid development of methods for the production of reactive nanofilms should be expected in the nearest future.

III. Reaction wave propagation in nanofilms

1. Initiation of reactions

To initiate a self-propagating reaction wave, it is necessary to locally heat a small region of the film to a particular temperature. As is known from the theory of combustion,[43] the ignition temperature is not a constant but is a kinetic parameter, *i.e.*, it depends not only on the composition of the mixture, but also on the heating rate, the rate of heat release and the level of heat losses to the environment. In powder mixtures, the ignition temperatures of the systems under consideration are often similar to the phase transition temperatures, for example, to the melting point of the low-melting reactant (at this temperature, the reaction rate sharply increases).

The initiation temperature of the reaction during slow heating can be most precisely determined by the DSC method.[44] The data obtained for the Ti—Al, Ni—Al and Nb—Al systems showed that the exothermic reaction in nanofilms starts at a temperature 300–400 K lower than the melting point of aluminium (933 K). For example, at a heating rate of 40 K min^{-1}, the reaction in the Ni/3Al film is initiated in the temperature range of 480–540 K;[15, 16, 44] in the Nb/Al, Nb/3Al and 2Nb/Al films, in the temperature range of 600–650 K.[23, 44] In the Ti/Al and Ti/3Al films, an intense heat release starts at 600–700 K.[20, 21] It was also noted that the initiation temperature of the reaction depends on the film thickness.

Experiments on combustion showed that self-ignition of Ti/Al and Ti/3Al films occurs in the temperature range of 600–650 K,[45] which is substantially lower than the ignition temperatures (the temperature of thermal explosion) of powder mixtures with a similar composition ((900–1000 K).[46]

From the practical point of view and taking into account the above-mentioned relatively low ignition temperatures, the initiation of reactions in nanofilms presents no difficulties. Different rather reliable methods, such as the ignition with a hot wire, a spark, a radiant flux or a laser pulse, are used. Nevertheless, in some cases it is necessary to know the precise dosage of the ignition energy, for example, when multilayer films are used for welding thin layers in microelectronics. Different methods for controlling the ignition energy of multilayer foils were considered.[47] An interesting laser ignition technique was documented.[48, 49] In these studies, Al/Pt foils were fired with a femtosecond laser pulse; the critical density of the radiant energy necessary for the initiation of the self-propagating process is 0.9–22 J cm^{-2}, a lower energy being required for films consisting of thinner layers.

After the local initiation, the reaction wave propagates through the film in the self-sustaining mode, and no external

supply of heat is required (see Fig. 1). The known characteristics of the propagation of these waves are considered below.

2. Metal – aluminium systems

Due to chemical self-heating, the reaction zone in multilayer films begins to glow orange (sometimes yellow). Hence, the reaction wave propagation can be detected with photodetectors or by high-speed video measurements.

Among films containing aluminium layers, the film of the Ni – Al system, in which the highest reaction propagation rates were observed, has the highest heat of reaction.[50–54] In the early study,[5] it has been already mentioned that the rate of the reaction front is ~ 4 m s^{-1}, and the total film thickness is at most 300 nm. More recently, the dependence of the propagation rate on the period d of a multilayer structure was studied.

Data on the rates of the reaction wave propagation in metal – aluminium nanofilms obtained by different authors are presented in Fig. 6. As can be seen from this figure, the propagation rate rapidly decreases with increasing d, because the diffusion path of the reactants increases and the rate of the heterogeneous reaction decreases.[50] The plot of the rate of the reaction wave propagation *vs* the layer thickness in metal – aluminium systems reaches the maximum for $d = 25-30$ nm. A decrease in the rate for thinner layers is associated with the fact that a very thin layer of the substance involved in the reaction is formed at the Ni/Al interface during sputtering; the layer thickness (*ca.* 0.1 – 1 nm) is constant and is independent of the thickness of the reaction layers.[50] For rather thick reaction layers, the weight fraction of the consumed substance is negligibly small, but this fraction increases as the period of the multilayer structure decreases, resulting in a lowering of the temperature and a decrease in the reaction rate. The fact that it is this layer of the consumed substance that causes a decrease in the reaction rate is evident also from a decrease in the reaction rate after annealing of samples (see curves *3–6* in Fig. 6); the thickness of this layer increases upon annealing.

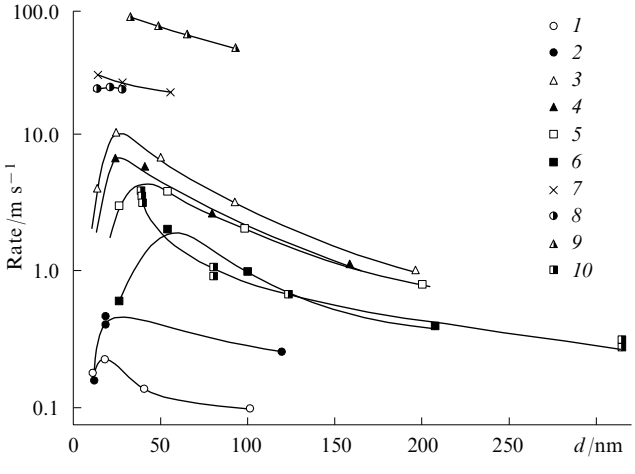


Figure 6. Plot of the rate of reaction wave propagation *vs* the period of a multilayer structure for different films.
(*1*) A Ti/Al film, the initial temperature was 473 K, ignition with a spark;[45] (*2*) *ibid*, ignition with a heated tungsten filament;[45] (*3*) a Ni/Al film after sputtering, the initial temperature was 298 K;[50] (*4*) *ibid*, after annealing at 423 K for 90 min;[50] (*5*) *ibid*, after annealing at 423 K for 6 h;[50] (*6*) *ibid*, after annealing at 423 K for 24 h;[50] (*7*) a 2Ni/Si film with a total thickness of 1.62 μm, the initial temperature was 298 K, ignition with a laser pulse;[55] (*8*) a 2Ni/Si film with a total thickness of 0.73 μm, the initial temperature was 298 K, ignition with a laser pulse;[55] (*9*) a Pt/Al film, the initial temperature was 298 K, ignition with a laser pulse;[48] (*10*) a Nb/Si film, the initial temperature was 298 K.[25]

A decrease in the rate of the reaction wave propagation with increasing layer thickness for Ni/Al and 3Ni/Al films was observed.[51] In this study, the ranges of the effective activation energies for the process were estimated (from 127.9 to 149.8 kJ mol^{-1} for Ni/Al and from 133.8 to 146.3 kJ mol^{-1} for 3Ni/Al). The question about the limiting layer thickness of reactants, for which self-sustaining reactions are possible, remains open. Since the preparation of rather thick (thicker than a micrometer) layers by sputtering methods presents difficulties, studies are performed with the use of foil stacks or rolls. The exothermic reaction in foils with thickness of ~ 50 μm was observed in the studies;[52, 53] however, the samples were additionally heated by passing the current. The studies with the use of rolling methods are presently underway.

A multilayer Ni/Al film was synthesised [54] by repeated cold rolling (this method is described in Section II); the total film thickness was ~ 200 μm; the layer thickness, according to the data on the microstructure, was $\sim 1-10$ μm. It should be noted that the layers were not continuous; more likely, they can be considered as having an anisotropic rather than multilayer microcstructure. After heating of the film in a flame for a few seconds, the relatively slow propagation of the first reaction front was observed, the film surface turning dark. Then the second reaction front with a red glow very rapidly propagated through the film. Unfortunately, the observed reaction waves were not quantitatively characterised in the study.[54]

The reactions in films of the Ti – Al system are less exothermic than the reactions of films of the Ni – Al system. For example, the adiabatic (in the absence of heat losses) combustion temperature of the Ni + Al composite is 1912 K, whereas this temperature is as low as 1519 K for the Ti + Al composite. Hence, it is not surprising that the rate of the reaction wave propagation is also lower for titanium – aluminium nanofilms. The dependence of this rate on the layer thickness [45] is similar in shape to the analogous plot for films of the Ni – Al system (the maximum is observed at 20 nm). It is interesting that the combustion rate depends on the mode of initiation of the reaction (see Fig. 6). The combustion of the same samples fired with a spark or a hot wire occurs at different rates, although no noticeable heating was observed in the initiation step. From the point of view of physical chemistry of combustion processes, this can be associated with several modes of the reaction wave propagation. It was also noted that the visual appearance of samples fired with a hot filament remains virtually unchanged during combustion, and their surface remains smooth. Samples fired with a spark become slightly corrugated; after combustion, their surface becomes rough. However, X-ray powder diffraction studies showed that the phase composition of the products is independent of the mode of initiation. This effect calls for further investigation.

Very high combustion rates were observed in films of the Pt – Al system.[48] The rates higher than 70 m s^{-1} suggest [48] that the measurements or published data are in error; nevertheless, these results are presented in Fig. 6. Here, the rate of the reaction wave propagation also gradually decreases with increasing layer thickness. The record high rates of the reaction wave propagation in Pt/Al nanofilms were confirmed in the study.[49] The measured rates varied from 20 to 90 (!) m s^{-1} depending on the double layer thickness and the total film thickness. The films were fired directly on the substrate (Si/SiO_2) at room temperature with a short laser pulse.

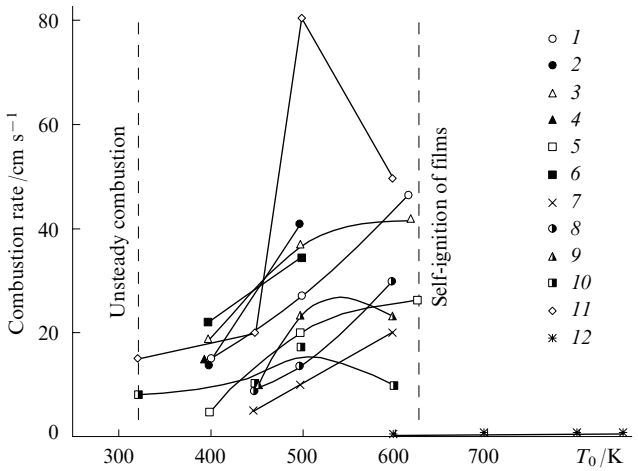


Figure 7. Plot of the combustion rate of multilayer foils *vs* the initial temperature.[46]
Curves: (*1–6*) ignition with a hot tungsten filament, (*7–11*) spark ignition, (*12*) comparison of the literature data for a powder Ti + Al mixture.[56] The Ti + Al composition: (*1*) 2200 layers, d = 18 nm; (*2*) 2200 layers, d = 28 nm; (*3*) and (*9*) 1350 layers, d = 18 nm; (*4*) 1350 layers, d = 28 nm; (*5*) 300 layers, d = 140 nm; (*6*) and (*10*) 4700 layers, d = 12 nm; (*7*) 300 layers, d = 100 nm; (*8*) 1000 layers, d = 40 nm. The Ti + 3 Al composition: (*11*) 300 layers, d = 120 nm.

For multilayer Ti/Al films, the plots of the combustion rates (*in vacuo*) *vs* the initial temperature were measured (Fig. 7). The steady-state combustion occurs in the initial temperature range of 400–600 K. Below 400 K, the steady-state reaction wave propagation in these films cannot be initiated. At the initial temperature of ~600 K, the self-ignition of films is observed. High-speed video measurements showed that the plot of the coordinate of the reaction front *vs* the time in the steady-state mode is nearly linear;[57] examples are given in Fig. 8.

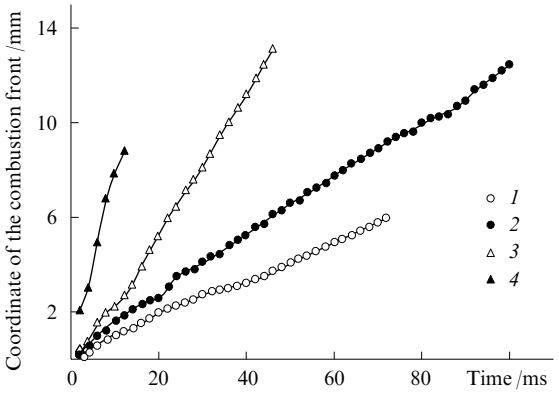


Figure 8. Plot of the coordinate of the reaction wave front *vs* the time.[57]
Foil: (*1*) Ti/Al, 46 layers with a layer thickness of 400 nm, T_0 = 700 K; (*2*) Ti/Al, 190 layers with a layer thickness of 100 nm, T_0 = 500 K; (*3*) Ti/Al, 190 layers with a layer thickness of 100 nm, T_0 = 600 K; (*4*) Ti/3Al, 400 layers with a layer thickness of 50 nm, T_0 = 300 K.

Measurments of the film temperature during the reaction is a complex experimental problem. Thermocouples introduce too large distortions into the process, whereas optical methods are inaccurate due to the lack of data on the radiation coefficients of films during the reaction. Nevertheless, the temperature profiles of the reaction waves were measured[45] with a photodetector calibrated on the same film (for the calibration, the film was heated by passing the current). The profiles are presented in Fig. 9. The accuracy of measurements is apparently similar to that of measurements with a brightness pyrometer.

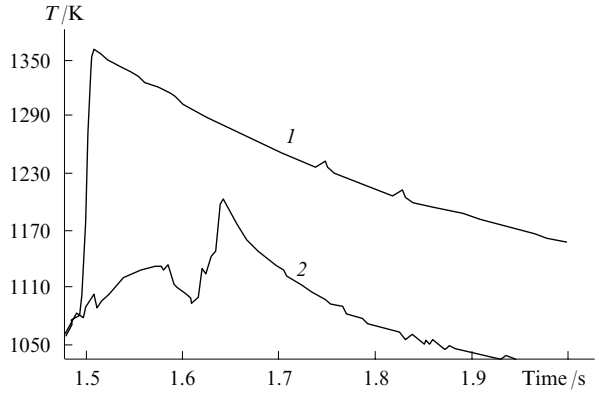


Figure 9. Temperature profiles for combustion of Ti/Al films in the steady-state (*1*) and oscillating (*2*) modes.[45]

3. Metal–silicon systems

Data on the rates of the reaction wave propagation in films of the Ni–Si system were obtained by high-speed video recording[55] (see curves *7* and *8* in Fig. 6) at a rate of 6000 images per second. Based on the video images reported in this publication, the width of the luminous zone was ~3–4 mm at a rate of the wave front propagation of 23 m s^{-1}; consequently, the luminescence time of the reaction zone was 0.13–0.17 ms. However, the analysis of the data from high-speed pyrometric measurements showed that the time of existence of the maximum temperature (1565 K) is substantially shorter. The results of pyrometric measurements[55] are presented in Fig. 10. The pyrometer was calibrated by the melting point of the Ni_2Si phase (1565 K). It should be noted that the data from the temperature measurements presented in Fig. 10 correspond to a fragment of the temperature profile of the process, because measurements in the wave front are absent, and the measurements in the cooling zone were not completed.

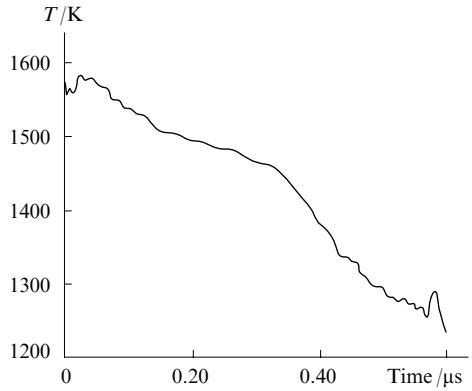


Figure 10. Temperature profile of the explosive siliconising wave in the multilayer 2Ni/Si film (d = 20.8 nm, the total foil thickness was 730 nm).[55]

The combustion rates of multilayer films of the Nb–Si system were measured using a a plurality of optical fibres that have been arrayed in a row along the direction of the reaction wave propagation, other ends of the fibres being fixed on the photodiode.[25] When the luminous front moves past a fibre, an electrical signal from the photodiode was fed to an oscillograph. As can be seen from Fig. 6 (curve *10*), the velocity of the reaction wave propagation in these films is lower than that in films of the Ni–Si system in spite of the fact that the adiabatic combustion temperature for films of the Nb–Si system should be much higher.

4. Other systems

Multilayer nanofilms were prepared also in the Ti–Si system conventionally used for investigations in the SHS region. However, data on the characteristics of the self-propagating process are very approximate. It was found that the reaction propagation occurs on a centimeter scale in a split second.[31]

An analogous situation was observed in films of several other systems, for example, of the Ni–Ti system. Powder Ni and Ti mixtures are well known in the theory and practice of SHS;[56] they are used for the synthesis of the intermetallide titanium nickelide having a shape memory effect. A new method for the synthesis of this compound from thin multilayer films (up to 100 alternating Ni and Ti layers) was developed;[58] however, nothing was said about the possibility of self-sustaining reactions in these films.

The reactions in thermite CuO_x–Al-type systems are highly exothermic (for example, the adiabatic combustion temperature for the 3 CuO + 2 Al composite is 2840 K). Multilayer films synthesised in this system by magnetron sputtering[26] have $d = 1000$ nm. The rate of the reaction wave propagation in films fired with a match was 1 m s^{-1}.

Studies on the combustion of relatively thin (~ 100 μm) layers of a powder Ti + B mixture[59] and porous Ti + 2 B films with a thickness of 230 μm, which were prepared from powders by the rolling method,[60, 61] are also of interest. The combustion rates of these composites are comparable with those of usual powder samples with the same composition (~ 0.1 m s^{-1}), and the microstructures of the starting films and the products are more similar to those of traditional powder composites than to those of multilayer films considered in the present review.

5. Reaction waves in very thin films

Studies of reaction waves in very thin films deposited on substrates can be considered separately. In these studies, the observed effects were assigned to SHS-type reaction waves. These films are characterised by a small total thickness (smaller than 200–300 nm), a small number of layers (most often, two layers) and the fact that the films are heated together with the substrate rather than are free-standing films (as opposed to the above-considered examples). In many cases, the wave propagation along films was visually observed. First studies were concerned with waves of film surface oxidation in air.[62, 63] More recently, waves of solid-state reactions were investigated.[28–30] For example, the reaction front propagation (the rate was ~ 0.01 m s^{-1}) was observed during heating of two-layer Ni/Al, Fe/Al and Co/Al films with a layer thickness of 30–100 nm *in vacuo* on glass or mica substrates.[29] The film mirror surface ahead of the front turns dull behind the front. Clearly, a very small film thickness, its contact with the substrate and a low rate of the wave front propagation cast doubt on the self-sustaining character of the process. More likely, the visible front is an isothermal line on the surface of the heated film such that the temperature along this line is equal to the temperature of a particular phase transition or reaction. This is evidenced by the decay of the reaction observed upon a lowering of the temperature of the substrate after the beginning of the wave propagation.[29]

According to the results of measurements with thermocouples,[28, 29] the temperatures of films were substantially higher than the temperatures of substrates. To measure the film temperature, a Pd layer was deposited onto the substrate followed by deposition of Fe and Al layers (the thickness of each layer was 50 nm), the Pd and Fe layers being used as the thermocouple. The sample was heated to 770 K at a rate of 10 K s^{-1}, and then the heater was switched off (the temperature of the heater was monitored with a chromel–copel thermocouple). Up to 660 K, the readings of both thermocouples were the same, but then the temperature of the film sharply rised to 1330 K. The SHS front propagation was observed[30] in two-layer Pt/Co films on a glass substrate heated to 770–840 K; quantitative data on the propagation rate were not reported. In films deposited on MgO substrates and containing up to 90 pairs of Pt and Co layers, no wave processes were observed.

In recent years, the existence of SHS waves in very thin layers of different compositions has been reported in several publications.[64–70] (We will return to these studies in the discussion of the possible mechanisms of nanoheterogeneous reactions.) However, data on the characteristic features of the propagation of the observed wave processes were not reported. Hence, the question as to whether the observed phenomena belong to self-propagating reaction waves remains open. Such results as multiple SHS[71, 72] where a certain visible front moves in one or another direction along the film surface depending on the heating or cooling rate also cast doubt on the chemical nature of some of the described 'waves'. The self-propagating high-temperature synthesis is known to lead to a sharp decrease in the free energy and the enthalpy of the system (this is the driving force of the process and leads to self-heating of the reaction medium) and an increase in the entropy. In most cases, these reactions are irreversible. The assumption that the reaction will go in the reverse direction and that the reagents mixed at the atomic level will be again separated into layers, is in contradiction with the fundamental principles of thermodynamics and the basic laws of physics and chemistry. Hence, presumably not all waves observed in superthin films are of chemical nature.

To summarise the data on the characteristic features of the reaction wave propagation in nanofilms, the following conclusions can be drawn. The number of these systems is much smaller than the number of known SHS systems suitable for the thin-film mode. The experimental conditions that influence the reliability of the results were determined in investigations of combustion processes (the establishment of steady-state conditions, precise measurements of the propagation rates and the temperature profiles and the exclusion of heating of the total sample during ignition) are often not fulfilled and are sometimes ignored in studies on thin films. This can be attributed to the fact that processes in multilayer films are studied primarily by researchers engaged in solid state physics and materials science, which are far from problems of physical chemistry of combustion. Evidently, this calls for the development of reliable procedures and methodology of studying reaction waves in nanofilms.

Apparently, the above-mentioned phenomena in superthin films are determined by several, rather than one, reaction

waves, as evidenced by a huge difference (four orders of magnitude) in the observed rates of the wave front propagation. To draw more definite conclusions, it is necessary to consider the mechanisms of propagation of different waves.

IV. Mathematical models for reaction wave propagation in nanofilms

Layer models (Fig. 11) have long been used in the theory of combustion, in particular, for the description of heterogeneous systems giving rise to condensed products.[73, 74] The starting medium supposedly consists of alternating layers of solid reactants. A layer of the solid product is formed at the interface of the reactants, and the thickness of this layer increases with time due to diffusion. The wave propagation process is described by the equation of heat conductivity with a source

$$c\rho\frac{\partial T}{\partial t} = \nabla(\lambda\nabla T) + \Phi(T, C) \tag{1}$$

and the equation of diffusion

$$\frac{\partial C}{\partial t} = \nabla(D\nabla C), \tag{2}$$

where c, ρ and λ are the average specific heat capacity, the density and the heat conductivity of the medium, respectively, T is the temperature, t is the time, Φ is the power of the heat source (the reaction heat release function), C is the reactant concentration (generally, the dimensionless concentration or the degree of conversion is used) and D is the diffusion coefficient for the key step of the heterogeneous diffusion-controlled reaction. The operator ∇ specifies the gradient in the two-dimensional space (a two-dimensional model is considered, see Fig. 11)

$$\nabla = \frac{\partial}{\partial x} + \frac{\partial}{\partial y}.$$

Assuming that the heat is released only in the diffusion-controlled reaction and ignoring heat losses, the heat source function can be written as follows:

$$\Phi(T, C) = Q\frac{\partial C}{\partial t} = Q\nabla(D\nabla C), \tag{3}$$

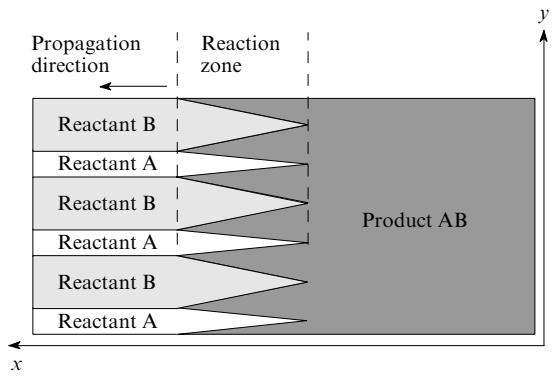


Figure 11. Layer combustion model.

where Q is the reaction heat. Equation (3) relates the equation of heat conductivity to the equation of diffusion.

Taking into account that the coefficient of thermal diffusitivity in solids

$$a = \frac{\lambda}{c\rho}$$

is much larger in magnitude than the diffusion coefficient, the following conclusions were drawn: the temperature distribution in the direction across the reaction layers can be considered to be uniform because it levels off much more rapidly than the concentrations; the heat propagation along the layers is much more rapid than the diffusion of the reactants; hence, the width of the heated zone ahead of the reaction wave front is substantially larger than the width of one reactant layer.

It can be approximately assumed that the heat transfer (the heat conductivity is assumed to be unchanged during the reaction) occurs only along the layers (the x axis in Fig. 11), whereas the diffusion occurs across the layers (the y axis). In this case, from the system of Eqns (1)–(3) we get

$$c\rho\frac{\partial T}{\partial t} = \lambda\frac{\partial^2 T}{\partial x^2} + \frac{1}{H}\int_0^H \Phi(T, C)\mathrm{d}y, \tag{4}$$

$$\Phi(T, C) = Q\frac{\partial}{\partial y}\left(D\frac{\partial C}{\partial y}\right). \tag{5}$$

Here, H is the total thickness of the multilayer film. The power of the heat source in Eqn (4) is uniformly distributed along the y axis (assuming that the temperature rapidly levels off across the film thickness). The average heat release power can be introduced

$$F(T, C) = QD\frac{\mathrm{d}C}{\mathrm{d}y} \tag{6}$$

and substituted as a function of the heat source into Eqn (4). It should be noted that, due to the constancy of the temperature along the y axis, it is possible to pass from partial derivatives to normal derivatives in Eqn (6). Finally, assuming that the reaction wave steadily propagates along the x axis at a constant rate U, Eqn (4) can be converted to the usual differential equation

$$\lambda\frac{\mathrm{d}^2 T}{\mathrm{d}x^2} - c\rho U\frac{\mathrm{d}T}{\mathrm{d}x} + F(T, C) = 0. \tag{7}$$

The boundary conditions are specified as follows:

$$x = -\infty \text{ at } T = T_0 = \text{const},$$

$$x = +\infty \text{ at } T = T_c = T_0 + \frac{Q}{c\rho} = \text{const}. \tag{8}$$

(T_c is the combustion temperature).

The system of Eqns (7) and (6) with the boundary conditions (8) describes a typical problem on the combustion wave propagation in the one-dimensional approximation. It can be seen that all characteristic features associated with the multilayer microstructure of the medium appeared to be accumulated solely in the source function (6), and the heat propagation occurs in such a way as if the medium were homogeneous. Hence, the equation for the rate of the steady-state wave

propagation in a layer model is, in essence, the same as that for the homogeneous combustion [75]

$$U \approx \frac{1}{c(T_c - T_0)} \left(2Q \int_{T_0}^{T_c} \lambda F(T, C) \mathrm{d}T \right)^{1/2}. \quad (9)$$

For the temperature dependence of the heat release function according to the Arrhenius law

$$F(T, C) \sim \exp\left(-\frac{E}{RT}\right),$$

it was demonstrated [75] that

$$U \sim \exp\left(-\frac{E}{2RT_c}\right). \quad (10)$$

Here, E is the activation energy of the limiting step of the process and R is the universal gas constant. An analysis of the layer model for the diffusion-controlled heterogeneous reaction [76–78] showed that the rate of wave propagation is inversely proportional to the sum of the thicknesses of two adjacent layers of the reactants (d). The equation for the combustion rate can be written as follows:

$$U = \frac{4\lambda T_c}{d} \left(\frac{3k_0 R}{E(T_c - T_0)} \right)^{1/2} \exp\left(-\frac{E}{2RT_C}\right), \quad (11)$$

where k_0 is the preexponential factor in the Arrhenius equation. Let us emphasise once again that the layer model has been initially used for the simplified description of heterogeneous mixtures having an irregular microstructure.

A layer model has found new use in the development of theoretical basics of the combustion of multilayer nanofilms, because the geometry of the model became consistent with the real microstructure of the reaction medium. To adapt the layer model to investigations of superthin layers, a partially mixed layer that exists in the starting sample at the interface between the reactants was included in the model.[79] It was assumed that the reactants are mixed within this non-zero thickness layer before the beginning of the reaction, and concentration gradients appear. The existence of the primary mixed layer was experimentally confirmed by transmission electron microscopy [79, 80] and DSC (a sharp decrease in reaction heat release was observed for reaction layers with thickness < 20 nm).[79] If the thickness of the mixed layer is small compared to the period of the layered structure, the rate of wave propagation is described by Eqn (11), where the activation energy and the preexponential factor should be substituted for E and k_0, respectively, into the bulk diffusion equation. If the period of the layered structure is smaller than 10–20 nm, the rate of reaction wave propagation sharply decreases under the effect of mixed layers. The results of calculations [50, 79] are consistent with the experimental data for films of the Ni–Al system (see Fig. 6). However, the layer model [79] includes a number of parameters, for example, the thickness of the mixed layer and the concentration profiles within this layer (linear, exponential, *etc.*), the activation energy of diffusion and the preexponential factor, which can be specified arbitrarily or in a rather wide range.

Studies of the stability of combustion propagation in multilayer nanofilms with respect to different parameters showed [81] that stability is lost and the combustion occurs in the autooscillation mode as the relative thickness of the mixed layer increases. An increase in the temperature of the environment (*i.e.*, a decrease in heat losses) leads to a decrease in the oscillation amplitude and stabilisation of combustion. The roughness of the reactive layers and the heterogeneity of their composition result in an increase in the oscillation amplitude. The existence of the oscillation mode of combustion in Ti/Al nanofilms was demonstrated experimentally by high-speed micro video recording.[45] Traces of autooscillations in the microstructure of the combustion product were studied in Zr/Al/(CuNi) (Ref. 82) and Ti/Al films.[57]

Heat losses to the environment can be of great importance in studies of thin foils. The influence of radiation and conductive heat losses on the combustion rate of multilayer foils was investigated theoretically.[83] In terms of the model used, an increase in heat losses leads to a decrease in the rate oscillation amplitude accompanied by an increase in the oscillation period. In the range of parameters characteristic of the Ni–Al system, the heat losses through radiation were demonstrated to have a much smaller effect on the combustion rate than conductive losses. In this study, the melting effect of a thin additional layer (Ni, Cu or Sn) on the foil surface, which can either suppress or enhance oscillation, was also taken into account. According to this model, melting of one of the reactants or products of the synthesis leads to a decrease in the average combustion rate.[84]

Thus, the results obtained with the use of the layer combustion model are, at first glance, in good agreement with experimental data. Two questions remain unanswered: (1) whether the above-mentioned assumptions are consistent with the real structures of the reaction medium and products; (2) whether the layer model can explain the unusually high rates of reaction wave propagation in nanofilms. The former question will be considered in the next section. To answer the latter question, simple estimates of the maximum rate can be made based on the theory of combustion.

The width of the heated zone ahead of the combustion wave front is equal to the ratio of the thermal diffusivity to the propagation rate a/U; consequently, the time of existence of the compound in this zone is

$$\tau_1 = \frac{a}{U^2}.$$

Generally, the reaction proceeds in a narrow zone near the maximum temperature; however, for an upper estimate of the combustion rate, the reaction diffusion will be assumed to proceed at the maximum rate throughout the period of time τ_1. According to the layer model (see Fig. 11), the time necessary for the mutual penetration (diffusion) of reactants is estimated from the equation

$$\tau_2 = \frac{d^2}{16D},$$

where

$$D = D_0 \exp\left(-\frac{E}{RT}\right)$$

is the diffusion coefficient and D_0 is the preexponential factor.

For the reaction wave to propagate at a rate U, the conditions $\tau_1 \geqslant \tau_2$ should be fulfilled. Hence, we get the equation for the maximum possible combustion rate

$$U_{\max} = \frac{4}{d}(aD)^{1/2}. \quad (12)$$

Consequently, in terms of the above-described assumptions, the maximum rate is determined by the thermal diffusivity and the diffusion coefficient. In the systems under consideration, the thermal diffusivity is in the range of $0.1-1.0$ cm^2 s^{-1}. For example, the thermal diffusivities for Al, Ni and Ti are 0.96, 0.22 and 0.09 cm^2 s^{-1}, respectively (presumably, the thermal diffusivity of nanolayers differs from that of bulk materials, being evidently smaller in nanolayers). The maximum propagation rate is observed (see Fig. 6) for $d = 25-30$ nm. To obtain the upper estimate, let us take the largest $a = 1$ cm^2 s^{-1} and the smallest $d = 25$ nm; substituting these parameters into the Eqn (12), we obtain

$$U_{\max} = 16 \times 10^5 D^{1/2}, \quad (13)$$

where the rate and the diffusion coefficient have the dimensionality m s^{-1} and m^2 s^{-1}, respectively. It can easily be calculated that the rate of reaction wave propagation equal to 72 m s^{-1} is possible provided the diffusion coefficient is at least 2×10^{-9} m^2 s^{-1}; the rate of 10 m s^{-1}, if $D \geqslant 4 \times 10^{-11}$ m^2 s^{-1}; the rate of 0.45 m s^{-1}, if $D \geqslant 8 \times 10^{-14}$ m^2 s^{-1}. The question is whether these values are consistent with the known diffusion coefficients in the corresponding systems.

In the Ti—Al system, the diffusion coefficient of aluminium in α-Ti is $\sim 5 \times 10^{-18}$ m^2 s^{-1} in the vicinity of the transition temperature for α-Ti → β-Ti (1155 K), and the diffusion coefficient of aluminium in β-Ti is $\sim 3 \times 10^{-14}$ m^2 s^{-1} at the same temperature.[85] The diffusion coefficients of Al and Ti atoms in the TiAl intermetallic phase are also of the order of 10^{-14} m^2 s^{-1}. This is quite sufficient for the explanation of the combustion rates up to 0.45 m s^{-1} observed in this system (see Fig. 6).

In the Ni—Al system, the NiAl phase has the highest melting point and is characterised by a wide homogeneity region at high temperatures. The diffusion coefficients of Al and Ni through the NiAl layer depend on the phase composition within the homogeneity region.[86] For example, the following mutual diffusion coefficients and the activation energies of diffusion were experimentally determined:[87] $D_0 = 4.8 \times 10^{-8}$ m^2 s^{-1} and $E = 115.9$ kJ mol^{-1} for the $NiAl_{1.17}$ phase and $D_0 = 10^{-4}$ m^2 s^{-1} and $E = 222$ kJ mol^{-1} for the $NiAl_{0.61}$ phase, respectively.[88] The mutual diffusion coefficients determined by extrapolation of these data to the adiabatic combustion temperature (1912 K) are 3.3×10^{-11} m^2 s^{-1} for $NiAl_{1.17}$ and 8.6×10^{-11} m^2 s^{-1} for $NiAl_{0.61}$. These values are also sufficiently large for an explanation of the combustion rate of the order of 10 m s^{-1} in Ni/Al nanofilms. It should be noted that the agreement between the calculated and experimental rates of reaction wave propagation was obtained [50, 79] for the diffusion coefficients of $(5-7) \times 10^{-10}$ m^2 s^{-1} at 1919 K. In spite of a number of assumptions, the above calculations overestimating the combustion rate (*i.e.*, underestimating the required diffusion coefficient) show that diffusion-controlled reactions can, in principle, provide the rates of reaction wave propagation in multilayer nanoscale systems of the order of $1-10$ m s^{-1}. A better agreement between the calculated and experimental data is achieved on the assumption that the diffusion coefficients in nanolayers are approximately an order of magnitude larger than those in bulk materials.

It is much more difficult to explain the rates of reaction wave propagation in the range from 30 to 90 m s^{-1}. For the Pt—Al system, the combustion temperature and the diffusion coefficient at this temperature are unknown. Hence, only approximate estimates can be used. Based on the heat of formation of PtAl (~ 100 kJ mol^{-1}),[48] the adiabatic combustion temperature can be estimated at ~ 1500 K, whereas the real temperature on a cold substrate should be lower. The diffusion coefficient of Al in Al_2Pt was determined only to 623 K.[89] The diffusion coefficient estimated by extrapolation of these data to 1500 K is $\sim 2 \times 10^{-11}$ m^2 s^{-1}. This is two orders of magnitude smaller than the required value in spite of all assumptions. An analogous situation is observed for the Ni—Si system. The adiabatic combustion temperature for the equimolar composition is 1265 K (equal to the melting point of NiSi). The temperature for the 2Ni/Si film determined by high-speed pyrometry [55] is 1565 K. The extrapolation of the diffusion coefficients determined for the low-temperature range (below 600 K) to this region gave [90] $D \sim 3 \times 10^{-12}-4 \times 10^{-10}$ m^2 s^{-1}. The diffusion coefficient of Ni in a thin $NiSi_2$ film determined [91] at 1273 K is 2.4×10^{-15} m^2 s^{-1}, and the diffusion coefficient of Al in this phase at 1223 K is 6.5×10^{-15} m^2 s^{-1}. Therefore, the observed combustion rates higher than 30 m s^{-1} can hardly be explained in terms of the layer combustion model based on the diffusion-controlled heterogeneous reaction.

In some studies, the exothermic waves with unusually high propagation rates were called explosive reactions (for example, explosive siliconising [55, 31]), and this process was referred to the known phenomenon of explosive crystallisation of metastable amorphous films. In spite of the fact that explosive crystallisation was described for the first time more than 150 years ago,[92] its mechanism remains unclear. Nowadays, this mechanism is being extensively studied. An analysis of the experimental and theoretical studies on the explosive crystallisation of amorphous substances in the context of the macrokinetics can be found, for example, in a review.[93] A detailed consideration of this process is beyond the scope of the present review. Let us only mention the main features of this process.

The explosive crystallisation is observed in amorphous films supercooled below the crystallisation temperature and existing in the metastable state. In the course of equilibrium crystallisation from a melt, the temperature increases to the melting point due to the heat released during the phase transition, which prevents further crystallisation. In metastable systems, the temperature is also raised due to the heat of crystallisation, which is accompanied by an increase in the atomic mobility, but the temperature of the system remains lower than the melting point of the crystalline phase. Atoms that are frozen in the amorphous state become mobile and are rearranged to form an equilibrium crystalline phase, the heat that is released accelerates crystallisation of the next portion of the substance and so on. The process becomes autocatalytic because crystallisation of a portion of the substance leads to acceleration of crystallisation of the amorphous phase and can propagate as a wave at a rate of tens of meters per second.

Of the available models of explosive crystallisation, only models involving the melting of an amorphous phase provide an explanation for the observed high propagation rates.[94, 95] The scheme of this process is presented in Fig. 12. At the temperature T_{ma}, melting of the amorphous phase (endothermic) is observed, a metastable melt supercooled with respect to the melting point of the crystalline phase T_{ca} is formed and the melt immediately crystallises to form a mono- or polycrystalline phase (the exothermic process). The heat transfer from the crystallisation boundary to the melting boundary is described by the equation of heat conductivity (taking into account the heat transfer to the substrate) analogous to the equation in the above-considered problem on the combustion wave. The

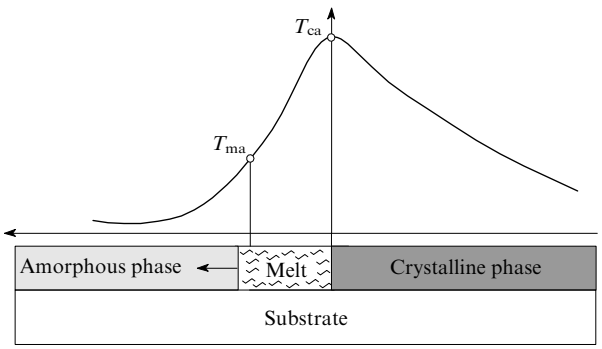


Figure 12. Scheme of explosive crystallisation in a thin film in the presence of a melt.[94]

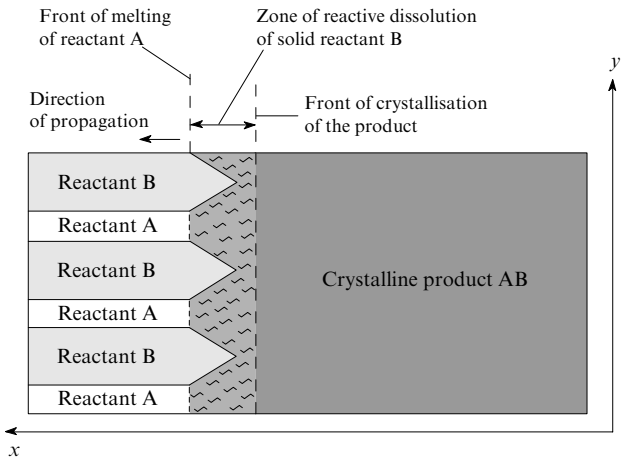


Figure 13. Scheme of a model for explosive chemical crystallisation in multilayer nanofilms.

difference is that in this case, the heat source function is not restricted by the requirement of diffusion mixing of reactants. Since the melting and crystallisation processes are diffusionless phase transitions, they depend only on the rate of heat supply to and heat removal from the interface between the solid phase and the melt. The heat of melting of the amorphous phase is 35 kJ mol^{-1} for silicon [94] and 23 kJ mol^{-1} for germanium.[95] The heat of crystallisation from a melt is 46 kJ mol^{-1} for silicon [94] and 37 kJ mol^{-1} for germanium.[95] These values are several times lower than the heat of reaction (for example, the reaction of Ti with Si is accompanied by the release of 164 kJ mol^{-1}), and the difference between the heat of melting of the amorphous phase and the heat of crystallisation of the melt, which determines the total power of the heat source, is ten times smaller than the heat of chemical reaction. According to the models under consideration, the explosive crystallisation can proceed in a narrow temperature range, and the thickness of the melt layer increases with increasing initial temperature of the substrate (see Fig. 12), resulting in a decrease in the combustion rate. This dependence is opposite to the expected and observed (see Fig. 7) dependence of the combustion rate of multilayer films on the initial temperature.[45]

Thus, the model of explosive crystallisation allows the explanation of the rates of wave propagation amounting up to tens of metres per second; however, the formation of chemical compounds after the wave propagation remains unexplained because the chemical reaction is absent in this model. It is worthwhile to develop a new model combining the features of the layer combustion model and the model of explosive crystallisation. The idea of this model is illustrated by Fig. 13. The melting wave propagates along the layer of the low-melting reactant A. The temperature at the melting front can be either equal to the equilibrium melting point of the compound A or lower than this temperature (by analogy with explosive crystallisation). The starting layer A is not necessarily amorphous because reduction of the melting point with respect to the equilibrium value is typical of many nanoscale compounds (both nanoparticles and thin films). The appearance of a melt leads to a sharp increase in the rate of the chemical reaction due to dissolution of the high-melting reactant B in the metastable liquid, the intensification of diffusion (the typical diffusion coefficients in melts are in the range of $\sim 10^{-9}-10^{-8}$ m^2 s^{-1}), wetting and the penetration of the melt through the grain boundaries. The fulfillment of the necessary condition that the melt should rapidly crystallise with heat evolution is the key factor in this hypothetical mechanism, as in the mechanism of explosive crystallisation. In the mechanism of the 'classical' explosive crystallisation, this condition is fulfilled due to the fact that the melting point of the amorphous phase is lower than the melting point of the crystalline phase (see above).

In multilayer nanofilms, the rapid crystallisation of melts can be associated with two factors. First, melting of nanocrystalline grains in a thin layer can proceed below the equilibrium melting point; in this case, the melt is metastable, as in the case of explosive crystallisation. The appearance of stable nuclei of the crystalline phase in this melt leads to the rapid propagation of the crystallisation front. Second, upon dissolution of the higher-melting reactant B, the composition of the melt changes, the crystallisation temperature sharply increases and the melt becomes metastable (supersaturated). In my opinion, this mechanism shows the best correlation with experimental data. In this case, the product AB_x rather than the pure compound A crystallises. The heat is released both during dissolution of the reactant B in the melt A and crystallisation of the product AB_x (intermediate or final). Since the heat of reaction is much higher than the heat of melting, it is sufficient that a small portion of the compound be consumed in the reaction for this wave to propagate. After crystallisation of the melt, the reaction proceeds by the solid-phase diffusion mechanism.

Many experimental features of combustion, including high rates of wave propagation, can be explained in terms of the hypothetical model of explosive chemical crystallisation; however, its further development and experimental verification are required (in particular, it is necessary to perform a detailed analysis of the structural and phase transformations during the exothermic reaction wave propagation in multilayer nanofilms).

V. Dynamics of phase and structural transformations in heterogeneous reactions in nanoscale systems

The evolution of the phase composition and the structure of thin-film systems under consideration was studied in sufficient detail (DSC, time-resolved X-ray diffraction, *etc.*) under slow heating. However, only scarce data on changes in these characteristics in the combustion wave were obtained for a number of systems. Based on the generalisation of experimental data, the two-step mechanism was suggested for the appearance and phase growth of the product.[44, 96] This mech-

anism is schematically presented in Fig. 14. In the first step, the nucleation of a new phase occurs at the interface between the reactants, and the grains grow until a continuous layer is formed. In the second step, this layer is developed in the direction perpendicular to the interface due to bulk diffusion of the reactants through the product. The questions about the phase compositions of the nuclei and the continuous layer and as to the consistency of the real microstructures with the simplified scheme (see Fig. 14) should be considered separately for each system.

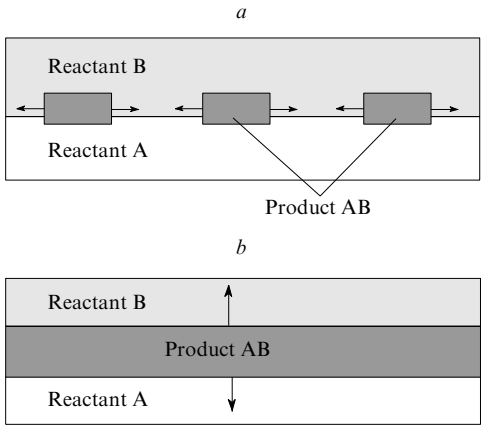


Figure 14. Scheme of the two-step mechanism of interactions between layers.[44,96]
(*a*) The nucleation and growth along the interface, (*b*) the layer growth of the product perpendicular to the interface.

System Ni – Al. The heating of Ni/3Al films, which were prepared by vacuum deposition ($d = 20-300$ nm), at a rate of 5 – 20 K min^{-1} initially afforded a solid solution, from which the $NiAl_3$ phase crystallised.[80] The intermetallic phase growth proceeded by the above-described two-step mechanism (see Fig. 14), the role of the first step being increased as d decreased, and the temperature of this step was shifted to lower temperatures (from 525 K for $d = 150$ nm to 480 K for $d = 10$ nm).

During heating of films containing from 48 at.% to 88 at.% Al ($d = 10$ and 20 nm), which were prepared by magnetron sputtering, at a rate of 40 K min^{-1}, the reaction also proceeded by the two-step mechanism.[14] The first step afforded the NiAl phase with a B2-type structure (the composition of this phase was $Ni_{37}Al_{63}$). In the case of films containing more than 63 at.% aluminium, the formation of the first phase was followed by the formation of the second phase, $NiAl_3$.

The heating of 2Ni/3Al films ($d = 12.5$, 25, 50, 100 or 200 nm), which were prepared by magnetron deposition, at a rate of 5 – 100 K min^{-1} afforded the metastable Ni_2Al_9 phase as the initial product when $d \geqslant 25$ nm; when $d = 12.5$ nm, the stable $NiAl_3$ phase appeared.[15] Based on the analysis of DSC curves, the following reaction pathway was suggested:

$$Al + Ni \longrightarrow Ni_2Al_9 + Ni,$$

$$Ni_2Al_9 + Ni \longrightarrow NiAl_3 + Ni,$$

$$NiAl_3 + Ni \longrightarrow Ni_2Al_3.$$

The microstructure of the first phase (Fig. 15 *a*)[16] is of interest. Unlike model views, this phase is not distributed as an even layer at the interface but consists of rounded grains and

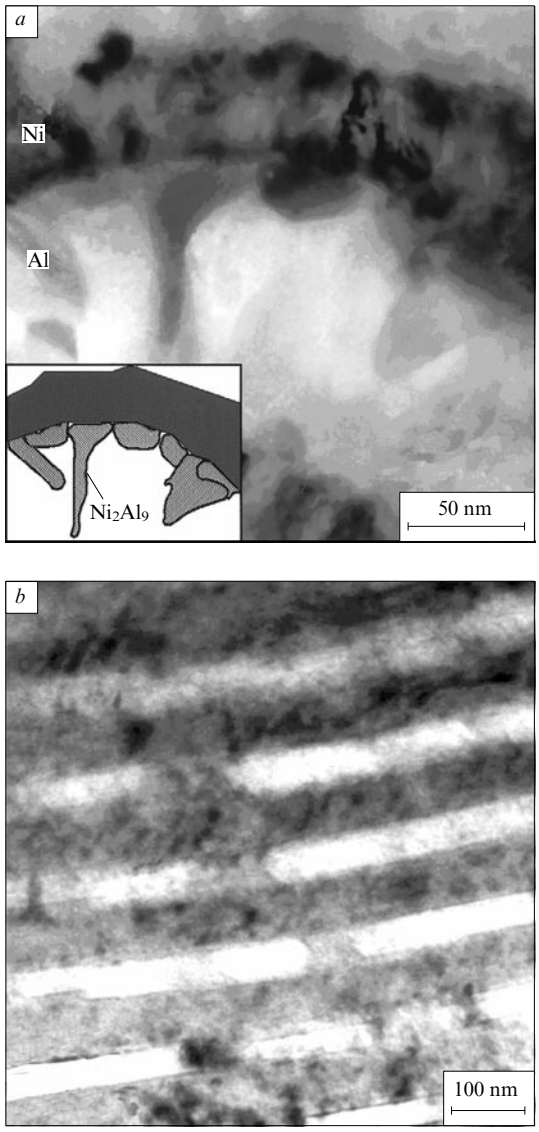


Figure 15. Microstructures of multilayer nanofilms in the reaction step.
(*a*) A Ni/Al sample after heating to 553 K (the growth of the Ni_2Al_9 phase occurs along the grain boundaries in the Al layer),[16] (*b*) a Ti/Al sample after heating to 1100 K (bridges of the product are formed along the grain boundaries).[21]

long 'fingers' that are formed, apparently, along aluminium grain boundaries.

A comparison of the results obtained under slow heating (20 K min^{-1}) and during combustion (4 m s^{-1}) of films of the Ni – Al system ($d = 15-300$ nm, vacuum deposition) showed that the reaction of 3Ni/Al films affords the Ni_3Al phase as the reaction product regardless of the reaction mode. However, the phase composition of the product for Ni/3Al films strongly depends on the reaction conditions.[5] The slow annealing gives $NiAl_3$ as the only phase, whose formation starts at 500 K, whereas the combustion affords the multiphase product $NiAl_3 + Ni_2Al_3 + Al$.

The role of the layer thickness of the reactants in the reaction can be revealed in more detail by studying multilayer foils prepared by the rolling method. Very thick layers (tens of micrometers) are characterised by the formation of several

layers of the product at the Ni/Al interface.[97,98] Generally, these layers include the NiAl and Ni_3Al phases. For thinner layers (of a micrometer scale), the two-step mechanism of interactions between layers giving rise to the primary $NiAl_3$ phase analogous to the reaction mechanism in nanofilms was described.[54]

System Ti – Al. Most of researchers believe that the slow heating initially affords the $TiAl_3$ phase, and this is true for both bulk [99] and thin-film [19,100] samples, as well as for a thin aluminium layer sputtered on a titanium substrate.[101] It should be noted that the disordered TiAl phase is initially formed in the temperature range of 800–850 K in Ti/Al films sputtered on a steel substrate [16] and then an equilibrium intermetallic TiAl phase is formed in the temperature range of 875–950 K (heating at a rate of 30 K min^{-1}). Differential scanning calorimetry studies of Ti/Al films with a thickness of 5 μm and having different structural periods also showed that the initial formation of the TiAl phase is followed by the formation of Ti_3Al when $d = 4–20$ nm and only when $d = 200$ nm the $TiAl_3$ phase is formed as the initial reaction product followed by the formation of TiAl and Ti_3Al.[20]

The most detailed information on the dynamics of changes in the phase composition and the structure immediately during the reaction can be obtained by synchrotron X-ray diffraction. The *in situ* synchrotron X-ray diffraction study of heating of Ti/3Al films (10 and 72 nm, 40 K min^{-1}) revealed a rather complex mechanism of the structure formation involving the formation of tetragonal and cubic modifications of $TiAl_3$ as the first and major phase, respectively.[18] The reaction in Ti/Al films with a period of layers from 8 to 1000 nm was studied by *in situ* synchrotron X-ray diffraction during heating at a rate of 12 K min^{-1} from room temperature to 1000 K.[22,35] Selected results are presented in Fig. 16. In films consisting of rather thick layers of reactants, the $TiAl_3$ phase is initially formed followed by the formation of TiAl as the final product (in the thickest layers, a peak of Ti_3Al or a Ti-based solid solution is also observed). In films with $d = 8$ nm, the reaction proceeds in one step, *i.e.*, the α-Ti phase is transformed into TiAl in a few seconds, which is accompanied by the sharp expansion and then the contraction of the crystal lattice.

The synchrotron X-ray diffraction study of the combustion of Ti/Al films ($d = 120$ nm, the total thickness is 20 μm) under helium led to the conclusion that the reaction proceeds in one step.[102] As can be seen from Fig. 17, the diffraction line of Ti(002) is transformed into the line of TiAl(111). The time of this transformation is shorter than < 0.04 s (the time resolution of the method). The results of the detailed study of changes in the line in the vicinity of the transition point are indicative of the rapid expansion followed by the contraction of the crystal lattice.

Investigations into the texture of polycrystalline multilayer Ti/Al films before and after combustion revealed an interesting phenomenon of the inherence of the crystallographic orientation of atomic layers in the combustion product.[8,21] Under conditions of sputtering or the isothermal reaction of thin films, the epitaxial layer growth of the product is a widely occurring phenomenon, but the epitaxial (with respect to the layers of the starting reactants) structure of the combustion products was found for the first time. It can be concluded that samples remember the initial orientation of the atomic planes even under conditions of rapid heating in the combustion wave, when one reagent undergoes melting.

During the reaction, the microstructure of Ti/Al films, like the microstructure of Ni/Al films, contains inclusions of the product oriented perpendicular to the layers and apparently along the grain boundaries (see Fig. 15*b*). The study [21] substantiated the suggestion that the nucleation and growth of such inclusions in thin films is energetically more favourable than the layer formation of the product along the interface between the reactants.

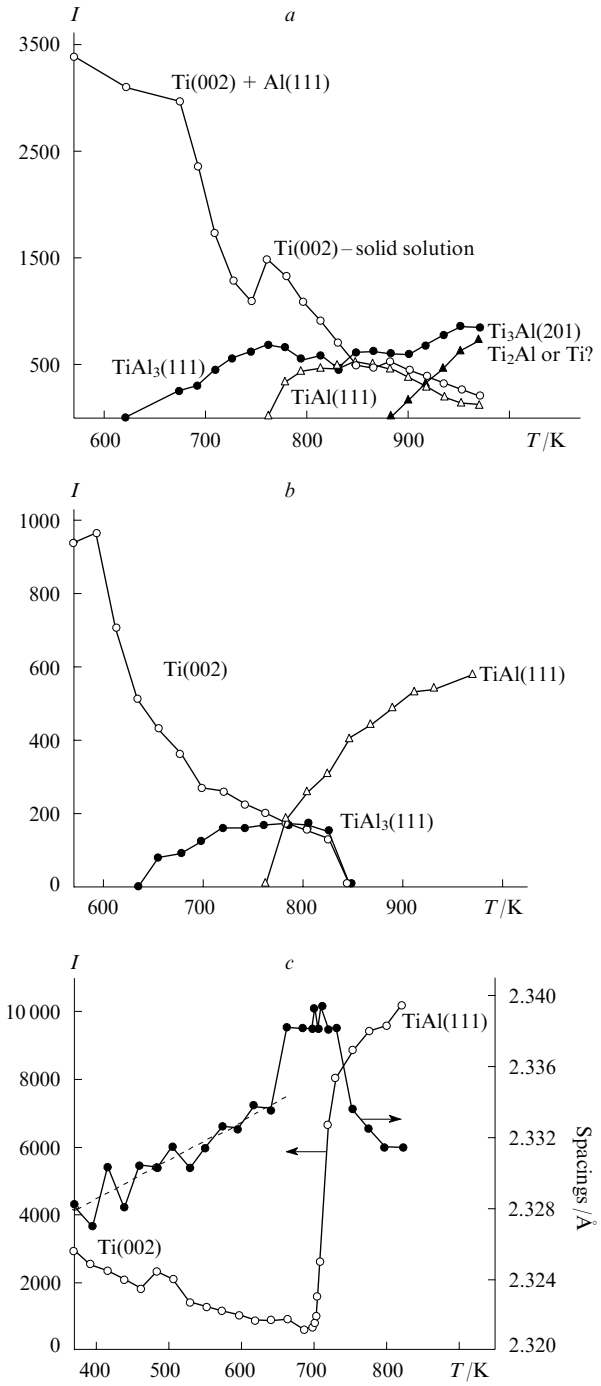


Figure 16. Dynamics of the phase formation in Ti/Al films during heating at a rate of 12 K min^{-1} according to the data from TRXRD-SR.[22,35] The period of layers is 780 (*a*), 50 (*b*) and 8 nm (*c*); *I* is the intensity of diffraction peaks.

System Nb – Al. This system (along with Ni – Si) served as the basis for the development of the two-step reaction model (see Fig. 14); the formation of a single-phase product was

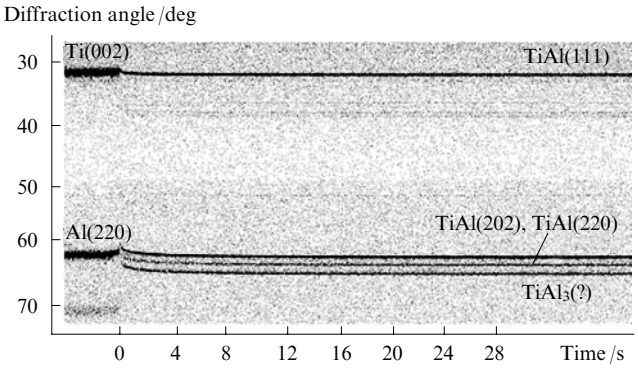


Figure 17. Dynamics of structural transformations during combustion of the Ti/3Al film in the autowave mode based on synchrotron X-ray diffraction data.[102]

accompanied by the appearance of two exothermic peaks in DTA and DSC thermograms.[96] The results of studies of Nb/3Al films (d = 72 nm, heating at a rate of 40 K min^{-1} to 973 K) by synchrotron X-ray diffraction confirmed the two-step mechanism, $NbAl_3$ being the only product of the heterogeneous reaction.[23] The concept of the two-step reaction mechanism was directly confirmed by studies of the evolution of the microstructure of films during the reaction.[12] Individual grains of the nucleating $NbAl_3$ phase (located predominantly in the vicinity of the grain boundaries) and continuous layers of this phase are seen in Fig. 18. Data on the structure formation for this system in the combustion mode are lacking.

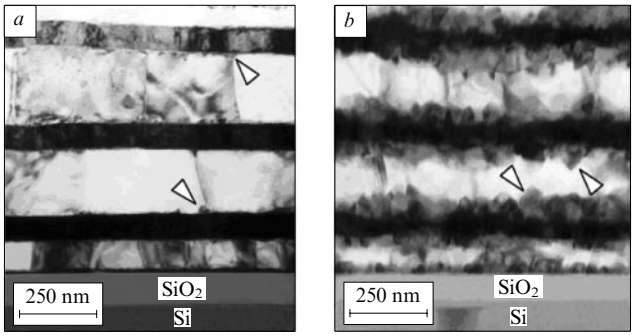


Figure 18. Formation of the product in films of the Nb – Al system.[12] The Nb and Al layers are dark and pale, respectively; grains of the primary product ($NbAl_3$) are indicated by arrows. Samples were heated at a rate of 40 K min^{-1} to 700 (*a*) and 900 K (*b*).

System Pt – Al. According to the data from DSC, X-ray diffraction and transmission electron microscopy, the amorphous $PtAl_2$ phase is initially formed in aluminium-rich thin films under slow heating and this phase grows layer-by-layer until platinum is completely consumed.[103] Then this phase reacts with aluminium that remains unconsumed to form particles of two crystalline phases similar in composition to $PtAl_5$, which are absent in the equilibrium phase diagram. These scarce data are insufficient for understanding of the record high rates of reaction wave propagation in this system.

System Co – Al. The slow heating of the 4Co/13Al film (d = 60 nm, the film thickness is 300 nm) initially affords the Co_2Al_9 phase followed by the formation of the quasicrystalline decagonal Co_4Al_{13} phase according to the above-mentioned two-step mechanism.[103] This system is of interest because its multilayer nanostructure can be transformed into a single-phase metastable quasicrystalline film with the decagonal atomic lattice stable in the temperature range from room temperature to 983 K. The SHS mode for films of this system has not yet been studied.

System Ni – Si. In the case of the molar composition of the 2Ni/Si film (the thickness of the Ni layer is equal to that of the Si layer, d = 14 – 100 nm, the film thickness is 70 – 500 nm, the heating rate is 1.25 – 20 K min^{-1}), only the Ni_2Si phase was obtained.[104] In foils with a period of the layered structure equal to 25 nm (or smaller), which were separated from the substrate, the explosive reaction was observed, which could be initiated not only by local heating but also by mechanical impact. The reaction was visually observed as a short yellow light flash and afforded Ni_2Si. The explosive reaction leads to a sharp increase in the size of crystalline blocks of the microstructure (Fig. 19, in the initial film, the silicon layers were amorphous). A more detailed study of this reaction showed that Ni_2Si is formed in both the amorphous and crystalline state, the amorphous phase being formed prior to the crystalline phase.[105] The formation of the Ni_2Si phase should be followed by the formation of the NiSi ($\sim$800 K) and $NiSi_2$ ($\sim$1000 K) phases in the case of a slow rise of the temperature and rather thick layers.

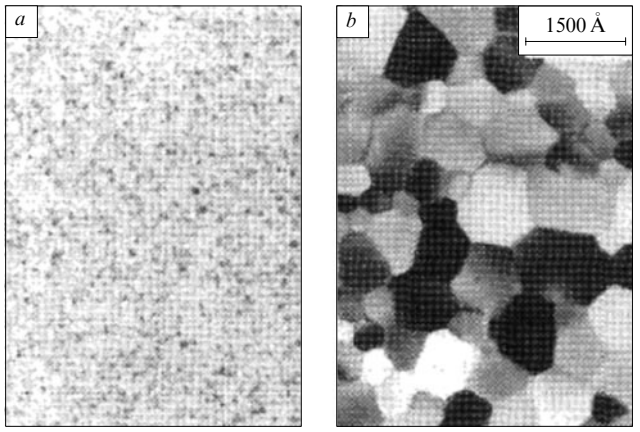


Figure 19. Microstructure of the multilayer Ni/Si film (d = 14 nm) in the initial state (*a*) and after explosive silication (*b*).[104]

System Nb – Si. After the reaction of the 11Nb/6Si film (26 at.% Si, d = 39 – 312 nm) in the combustion mode, the combustion product consisted of Nb_5Si_3 and Nb.[25]

System Ti – Si. In the study,[31] the formation of amorphous silicide layers, similar in chemical composition to TiSi, under slow heating was opposed to the formation of equilibrium crystalline silicides, mainly of the Ti_5Si_3 phase, as a result of the self-propagating exothermic reaction characterised by a high local temperature. After the SHS reaction, the film surface acquires the maple leaf macrostructure. The preparation of silicide phases by slow annealing initially affords the metal-rich phases M_5Si_3 and MSi, whereas the MSi_2 phases are formed in the subsequent step (where M = Ti, Zr, V or Hf).[106]

System Ti – Ni. The annealing of multilayer nanofilms of this system in different modes afforded the TiNi phase with the shape memory effect.[58]

To summarise the published data on the structure and phase formation in reactions in nanofilms, two conclusions can be drawn. First, the mechanism of reactive structuring strongly changes in going from macroscopic systems to nanoscale systems. Second, data on the structure formation are scarce and sometimes contradictory even for known systems, not to mention that most of known SHS systems were not obtained in the thin-film state.

VI. Practical application

Studies of reaction waves in multilayer nanofilms have been started in recent years; however, the results of these studies have already found use in industrial technologies. The welding and soldering of various materials and goods under special conditions are apparently the most advanced technologies.

It was reported [107] that metal glasses (amorphous metal alloys) of the composition $Zr_{57}Ti_5Cu_{20}Ni_8Al_{10}$ can be welded with the use of a multilayer Ni/Al nanofoil (to be more precise, Inconel 600/aluminium, because nickel-based layers contain also iron and chromium). A foil was pressed between two plates made of an amorphous alloy and the reaction was initiated by passing the current with a voltage of 30 V. The shear strength of the product was as high as 480 MPa. The Ni/Al foils have found use for joining (soldering) parts made of titanium alloys,[108] as well as of stainless steal and aluminium.[109] The scheme of the technology is presented in Fig. 20. The low-melting AuSn and AgSn alloys are used as solders;[109] higher-melting copper-silver solid solders [108] and amorphous solders [110] have also found use.

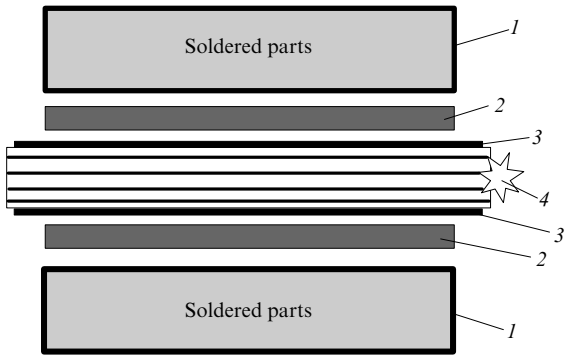


Figure 20. The scheme of welding of various materials using reactive multilayer nanofoils.
(*1*) A Ni or Au coating, (*2*) a solder (AuSn or AgSn) layer, (*3*) an Incusil layer, (*4*) spark ignition of a multilayer nanofilm.
The composition of the Incusil layer (solid solder) (mass %): Ag — 59, Cu — 27.25, In — 12.5, Ti — 1.25.

The advantage of this technology is that the heat pulse from the reacting foil is precisely dosed, due to which the thermal effect on the soldered materials and their microstructure is reduced to minimum. The influence of the compression pressure [109] and the thermal physical properties of components [111] on the strength of soldering and the structure of soldered parts was investigated. The thermal effect was examined using an infrared camera (thermal visor).[112] The results of all investigations showed that this technology can be used for soldering of metal glasses with their amorphous structure being unchanged, for soldering of very sensitive components of microelectronic technology, *etc.*¶ under difficult conditions, where the use of other techniques presents problems. The development of this technology is funded by U.S. Government Grants (the National Science Foundation and the U.S. Army Small Business Innovation Research Program) giving 5 million dollars. This technology is also awarded by the scientific and technological journals *R&D Magazine* and *NASA Nanotech Briefs Magazine*. Nowadays, the commercial production is 270 m^2 nanofilms per month (depending on the film thickness and requirements of consumers), and it gradually increases.

The second field of application is based on the use of such characteristic features of nanofilms as the easy initiation, high reaction rates and high combustion temperatures. The Reactive NanoTechnologies Company reported the application of films for the rocket fuel ignition, flares and igniters. Data on the possible use of reactive nanofilms in car air bags, for the rapid and reliable ignition of gas-generating mixtures, were published. However, the data in these field are scarce.

The TiNi nanofoils with the shape memory effect synthesised by heterogeneous reactions [58] hold great promise for the use in so-called microelectromechanical systems,[113] including nanodevices. Many known reactions in nanofilms can find use for the design of protection (chemically stable, durable, *etc.*) coatings. Presumably, the practical use of reaction waves in multilayer nanofilms is now in prospect.

VII. Conclusion

Based on the critical analysis of publications on exothermic reaction waves in multilayer nanofilms, the existence of the following three classes of wave processes can be noted.

1. Self-propagating reaction waves (thin-film SHS) at rates from 0.1 to 10 m s^{-1}. Generally, this process is observed in films separated from an inert substrate. It is accompanied by bright luminescence and considerable heat release, which allows the use of this process in welding technologies. The layer combustion model adequately describes the dependence of the combustion rate on the layer thickness, although the diffusion coefficients for layers should be taken higher than for bulk materials.

2. Very fast reaction waves (at rates in the range of 10 – 100 m s^{-1}). Generally, they are initiated by a laser pulse in films deposited on a cold substrate. The reaction is accompanied by a short light flash. Apparently, the mechanism of this process involves the explosive crystallisation. A model of explosive chemical crystallisation was suggested for an explanation of such high rates of wave propagation.

3. Very slow waves in films with a thickness smaller than a micrometer, which are heated together with a substrate. The waves show no luminescence but can be observed in reflected light due to changes in the reflectivity of the film surface. The rates of their propagation are lower than 0.01 m s^{-1}. In some

¶ In 2001, the Reactive NanoTechnologies Company was founded in the USA (for detailed information, see www.rntfoil.com). This company has monopoly in the use of the patented technology of soldering parts with reactive multilayer nanofoils. In 2004, this technology was included in the National Nanotechnology Initiative Strategic Plan developed by the National Science and Technology Council, Committee on Technology, the Subcommittee on Nanoscale Science, Engineering, and Technology. In this plan, it was noted that a broad range of users, from manufacturers of computer chips and printed-circuit boards to manufacturers of components for aerospace technology, are interested in the new method for soldering (see http://www.nano.gov/NNI_Strategic_Plan_2004.pdf).

cases, the wave propagation in the opposite direction is observed upon cooling; repeated heating gives rise to the repeated wave. Apparently, most of these phenomena are associated with the movement of the boundary of a particular phase or structural transition caused by heating of the substrate/film system.

The characteristics and the mechanism of the reaction wave propagation in nanofilms are poorly studied. The development of diagnostic methods for this process (the determination of the local and global propagation rates, the temperature profile of the wave, *etc*.) to obtain more comprehensive data on the characteristic features of the reaction wave propagation in nanofilms of different composition and with different structures is one of the most important experimental problems. The inclusion of real reaction pathways and mechanisms of heterogeneous reactions in nanoscale systems reveled by modern methods of investigation (synchrotron X-ray diffraction, high-resolution electron microscopy, *etc*.) instead of the idealised mechanism of reaction diffusion is promising for improvement of the theoretical models of this phenomenon. Evidently, studies of reactive multilayer nanofilms will help in studying heterogeneous reactions in nanoscale systems, if the relationship between the reaction mechanism and the macroscopic behaviour of the reaction wave will be established.

The above-considered phenomena have found use in various technologies, in particular, in a new method of welding of materials and for the design of initiating devices for different purposes. Apparently, these phenomena will find wider practical applications when new fundamental knowledge on the process will be obtained.

This review has been written with the financial support of the Russian Foundation for Basic Research (Project Nos 07-03-00 753 and 06-03-22 000-PICS) and the INTAS (Project No. 4103). I thank the National Council for Scientific Research (CNRS, France) and the Carnot Institute of Burgundy (Institut Carnot de Bourgogne, Dijon, France) for giving me the possibility to work with scientific databases.

References

1. A G Merzhanov, I P Borovinskaya *Dokl. Akad. Nauk SSSR* **204** 366 (1972) [a]
2. A G Merzhanov *Usp. Khim*. **72** 323 (2003) [*Russ. Chem. Rev*. **72** 289 (2003)]
3. T S Dyer, Z A Munir, V Ruth *Scr. Metall. Mater*. **30** 1281 (1994)
4. U Anselmi-Tamburini, Z A Munir *J. Appl. Phys*. **66** 5039 (1989)
5. E Ma, C V Tompson, L A Clevenger, K N Tu *Appl. Phys. Lett*. **57** 1262 (1990)
6. US P. 5538795 (1996)
7. *Thin Films. Interdiffusion and Reactions* (Eds J Poate, K Tu, J Mayer) (New York: Wiley, 1978)
8. A E Grigoryan, N G Elistratov, D Yu Kovalev, A G Merzhanov, A N Nosyrev, V I Ponomarev, A S Rogachev, V I Khvesyuk, P A Tsygankov *Dokl. Akad. Nauk* **381** 368 (2001) [a]
9. N G Elistratov, A N Nosyrev, V I Khvesyuk, P A Tsygankov *Prikl. Fiz*. **3** 8 (2001) [b]
10. X Chu, M S Wong, W D Spoul, S L Rohde, S A Barnett *J. Vac. Sci. Technol., A* **10** 1604 (1992)
11. P C Yashar, W D Sproul *Vacuum* **55** 179 (1999)
12. G Lucadamo, K Barmak, D T Carpenter, J M Rickman *Acta Mater*. **49** 2813 (2001)
13. A C Lewis, D Josell, T P Weihs *Scr. Mater*. **48** 1079 (2003)
14. A E Grigoryan, E V Illarionova, B A Loginov, A N Nosyrev, A S Rogachev, N V Sachkova, P A Tsygankov, I Yu Yagubova *Izv. Vyssh. Uchebn. Zaved., Tsvetn. Metall*. (5) 31 (2006) [c]
15. C Michaelsen, G Lucadamo, K Barmak *J. Appl. Phys*. **80** 6689 (1996)
16. K J Blobaum, D Van Heerden, A J Gavens, T P Weihs *Acta Mater*. **51** 3871 (2003)
17. C Coelho, A S Ramos, B Trindade, M T Vieira, J V Fernandes, M Vieira *Surf. Coat. Technol*. **120 – 121** 297 (1999)
18. G Lukadamo, K Barmak, C Lavoie, C Cabral Jr, C Michaelsen *J. Appl. Phys*. **91** 9575 (2002)
19. A S Ramos, R Calinas, M T Vieira *Surf. Coat. Technol*. **200** 6196 (2005)
20. A S Ramos, M T Vieira *Surf. Coat. Technol*. **200** 326 (2005)
21. J-C Gachon, A S Rogachev, H E Grigoryan, E V Illarionova, J-J Kuntz, D Yu Kovalev, A N Nosyrev, N V Sachkova, P A Tsygankov *Acta Mater*. **53** 1225 (2005)
22. I Yu Yagubova, A E Grigoryan, A S Rogachev, M R Sharafutdinov, B P Tolochko, P A Tsygankov, A N Nosyrev *Izv. Akad. Nauk, Ser. Fiz*. **71** 278 (2007) [d]
23. G Lukadamo, K Barmak, S Hyun, C Cabral Jr, C Lavoie *Mater. Lett*. **39** 268 (1999)
24. A S Rogachev, J-C Gachon, T Weihs, in *SHS 2005 the VIII International Symposium on Self-Propagating High-temperature Synthesis. (Book of Abstracts)*, Quartu S Elena, Italy, 2005 p. 92
25. M E Reiss, C M Esber, D Van Heerden, A J Gavens, M E Williams, T P Weihs *Mater. Sci. Eng. A* **261** 217 (1999)
26. K J Blobaum, M E Reiss, J M Plitzko, T P Weihs *J. Appl. Phys*. **94** 2915 (2003)
27. K J Blobaum, A J Wagner, J M Plitzko, D Van Heerden, D H Fairbrother, T P Weihs *J. Appl. Phys*. **94** 2923 (2003)
28. V G Myagkov, L E Bykova *Dokl. Akad. Nauk* **354** 777 (1997) [a]
29. V G Myagkov, V S Zhigalov, L E Bykova, V K Mal'tsev *Zh. Tekh. Fiz*. **68** (10) 58 (1998) [e]
30. V G Myagkov, L A Li, L E Bykova, I A Turpanov, P D Kim, G V Bondarenko *Fiz. Tv. Tela* **42** 937 (2000) [f]
31. E Ma *Mater. Sci. Eng. A* **398** 60 (2005)
32. S Kikuchi, H Kuwahara, N Mazaki, S Urai, H Miyamura *Mater. Sci. Eng. A* **234 – 236** 1114 (1997)
33. H Sieber, J S Park, J Weissmuller, J H Perepezko *Acta Mater*. **49** 1139 (2001)
34. R J Hebert, J H Perepezko *Scr. Mater*. **50** 807 (2004)
35. A S Rogachev, J-C Gachon, H E Grigoryan, E Illekovv, N F Kochetov, F N Nosyrev, N V Sachkova, J C Schuster, M R Sharafutdinov, N F Shkodich, B P Tolochko, P A Tsygankov, I Y Yagubova *Nucl. Instrum. Meth. Phys. A* **575** 126 (2007)
36. N F Shkodich, N A Kochetov, A S Rogachev, D Yu Kovalev, N V Sachkova *Izv. Vyssh. Uchebn. Zaved., Tsvetn. Metall*. (5) 44 (2006) [c]
37. F Bernard, E Gaffet *Int. J. Self-Propag. High-Temp. Synth*. **10** (2) 109 (2001)
38. T Grigorieva, M Korchagin, N Lyakhov *KONA Powder Part*. **20** 144 (2002)
39. A Mishra, J P Hirth, R G Hoagland, J D Embury, H Kung *Acta Mater*. **52** 2387 (2004)
40. R Miyazaki, S Kainuma, K Hisatake, T Watanabe, N Fukumuro *Electrochim. Acta* **44** 3713 (1999)
41. H Zamah, S Ikeda, Y Ueda *IEEE Trans. Magn*. **33** 3517 (1997)
42. N Fijita, M Izaki, M Inoue *J. Magn. Magn. Mater*. **300** e350 (2006)
43. Ya B Zel'dovich, D A Frank-Kamenetskii *Zh. Fiz. Khim*. **12** 100 (1938) [g]
44. C Michaelsen, K Barmak, T P Weihs *J. Phys. D: Appl. Phys*. **30** 3167 (1997)
45. A S Rogachev, A E Grigoryan, E V Illarionova, I G Kanel', A G Merzhanov, A N Nosyrev, N V Sachkova, V I Khvesyuk, P A Tsygankov *Fiz. Goren. Vzryva* **40** (2) 45 (2004) [h]
46. A G Merzhanov, E B Pis'menskaya, V I Ponomarev, A S Rogachev *Dokl. Akad. Nauk* **363** 203 (1998) [a]
47. WO/2005/005092
48. Y N Picard, D P Adams, J A Palmer, S M Yalisove *Appl. Phys. Lett*. **88** 144102 (2006)
49. D P Adams, M A Rodrigues, C P Tigges, P G Kotula *J. Mater. Res*. **21** 3168 (2006)
50. A J Gavens, D Van Heerden, A B Mann, M E Reiss, T P Weihs *J. Appl. Phys*. **87** 1255 (2000)

51. T S Dyer, Z A Munir *Metall. Mater. Trans. B* **26** 603 (1995)
52. V A Shcherbakov, A S Shteinberg, Z A Munir *Combust. Sci. Technol.* **169** 1 (2001)
53. V A Shcherbakov, A S Shteinberg, Z A Munir *Dokl. Akad. Nauk* **364** 647 (1999) [a]
54. X Qiu, J Wang *Scr. Mater.* **56** 1055 (2007)
55. L A Clevenger, C V Tompson, K N Tu *J. Appl. Phys.* **67** 2894 (1990)
56. V I Itin, Yu S Naiborodenko *Vysokotemperaturnyi Sintez Intermetallicheskikh Soedinenii* (High-temperature Synthesis of Intermetallic Compounds) (Tomsk: Tomsk State University, 1989)
57. A S Rogachev, N A Kochetov, I Yu Yagubova, H E Grigoryan, N V Sachkova, A N Nosyrev, P A Tsygankov *Int. J. Self-Propag. High-Temp. Synth.* **13** 285 (2004)
58. T Lehnert, S Tixier, P Böni, R Gotthardt *Mater. Sci. Eng. A* **273**–**275** 713 (1999)
59. M A Ponomarev, V A Shcherbakov, A S Shteinberg *Dokl. Akad. Nauk* **340** 642 (1995) [a]
60. S G Vadchenko, I P Borovinskaya, A G Merzhanov *Dokl. Akad. Nauk* **408** 123 (2006) [a]
61. S G Vadchenko, I P Borovinskaya, A G Merzhanov *Izv. Vyssh. Uchebn. Zaved., Tsvetn. Metall.* (5) 36 (2006) [c]
62. V G Myagkov, N V Baksheev *Pisma Zh. Tech. Fiz.* **18** (6) 14 (1992) [i]
63. V G Myagkov, L I Kveglis, G I Frolov, V S Zhigalov *J. Mater. Sci. Lett.* **13** 1284 (1994)
64. V G Myagkov, L E Bykova, G N Bondarenko *Pisma Zh. Tech. Fiz.* **32** (19) 5 (2006) [i]
65. V G Myagkov, L E Bykova V S Zhigalov, A I Pol'skii, G N Bondarenko *Dokl. Akad. Nauk* **371** 763 (2000) [a]
66. V G Myagkov, L E Bykova, L A Li, I A Turpanov, G N Bondarenko *Dokl. Akad. Nauk* **382** 463 (2001) [a]
67. V G Myagkov, L E Bykova, G N Bondarenko *Dokl. Akad. Nauk* **388** 46 (2003) [a]
68. V G Myagkov, L E Bykova, G N Bondarenko *Dokl. Akad. Nauk* **390** 35 (2003) [a]
69. V G Myagkov *Dokl. Akad. Nauk* **392** 54 (2003) [a]
70. V G Myagkov, L E Bykova *Dokl. Akad. Nauk* **396** 187 (2004) [a]
71. V G Myagkov *Dokl. Akad. Nauk* **364** 330 (1999) [a]
72. V G Myagkov, L E Bykova, G N Bondarenko *Zh. Eksp. Teor. Fiz.* **88** 963 (1999) [j]
73. A P Aldushin, B I Khaikin *Fiz. Goren. Vzryva* **10** 313 (1974) [h]
74. A P Hard, P V Phung *Combust. Flame* **21** 77 (1973)
75. D A Frank-Kamenetskii *Diffuziya i Teploperedacha v Khimicheskoi Kinetike* (Diffusion and Heat Transfer in Chemical Kinetics) (Moscow: Nauka, 1967)
76. R Armstrong *Combust. Sci. Technol.* **71** 155 (1990)
77. R Armstrong, M Koszykowski, in *Combustion and Plasma Synthesis of High-Temperature Materials* (Eds Z A Munir, J B Holt) (New York: VCY, 1990) p. 88
78. R Armstrong *Metall. Trans. A* **23** 2339 (1992)
79. A B Mann, A J Gavens, M E Reiss, D Van Heerden, G Bao, T P Weihs *J. Appl. Phys.* **82** 1178 (1997)
80. E Ma, C V Thompson, L A Clevenger *J. Appl. Phys.* **69** 2211 (1991)
81. S Jayaraman, O M Knio, A B Mann, T P Weihs *J. Appl. Phys.* **86** 800 (1999)
82. J C Trenkle, J Wang, T P Weihs, T C Hufnagel *Appl. Phys. Lett.* **87** 153108 (2005)
83. S Jayaraman, A B Mann, M Reiss, T P Weihs, O M Knio *Combust. Flame* **124** 178 (2001)
84. E Besnoin, S Cerutti, O M Knio, T P Weihs *J. Appl. Phys.* **92** 5474 (2002)
85. Y Mishin, C Herzig *Acta Mater.* **48** 589 (2000)
86. C Herzig, S Divinski *Intermetallics* **12** 993 (2004)
87. H Wei, X Sun, Q Zheng, H Guan, Z Hu *Acta Mater.* **52** 2645 (2004)
88. T Helander, J Agren *Acta Mater.* **47** 1141 (1999)
89. P Gas, J Labar, G Glunget, A Kovacs, C Bergman, P Barna *J. Appl. Phys.* **90** 3899 (2001)
90. H Takai, K N Tu *Phys. Rev. B* **38** 8121 (1988)
91. S I Sidorenko, S M Voloshko, Yu M Makogon, O P Pavlova, S O Zamul'ko, A V Mogilatenko, G Beddis *Metallofiz. Noveish. Tekhnol.* **27** 1529 (2005) [k]
92. G Gore *Philos. Mag.* **9** 73 (1855)
93. V A Shklovskii, V M Kuz'menko *Usp. Fiz. Nauk* **157** 311 (1989) [*Physics Uspekhi* **32** 163 (1989)]
94. H-D Geiler, E Glaser, G Gltz, M Wagner *J. Appl. Phys.* **59** 3091 (1986)
95. C Grigoropoulos, M Rogers, S H Ko, F F Golovin, B J Matkowsky *Phys. Rev. B* **73** 184125 (2006)
96. K R Coffey, L A Clevenger, K Barmak, D A Rudman, C V Tompson *Appl. Phys. Lett.* **55** 852 (1989)
97. H Wang, J Han, S Du, D O Northwood *Mater. Sci. Eng. A* **445**–**446** 517 (2007)
98. H Wang, J Han, S Du, D O Northwood *Metall. Mater. Trans. A* **38** 409 (2007)
99. F J J van Loo, G D Rieck *Acta Metall.* **21** 61 (1973)
100. R W Bower *Appl. Phys. Lett.* **23** 99 (1973)
101. S E Romankov, B N Mukashev, E L Ermakov, D N Muhamedshina *Surf. Coat. Technol.* **180**–**181** 280 (2004)
102. A S Rogachev, J-C Gachon, H E Grigoryan, A N Nosyrev, P A Tsygankov, J C Schuster, D Vrel *Nucl. Instrum. Meth. Phys. Res. A* **543** 175 (2005)
103. C Bergman, P Gas, D Mangelinck *J. Electroanal. Chem.* **573** 71 (2004)
104. L A Clevenger, C V Tompson, R C Cammarata, K N Tu *Appl. Phys. Lett.* **52** 795 (1988)
105. L A Clevenger, C V Tompson *J. Appl. Phys.* **67** 1325 (1990)
106. O Chaix-Pluchery, B Chenevier, I Matko, J P Sénateur, F La Via *J. Appl. Phys.* **96** 361 (2004)
107. A J Swiston, Hufnagel, T P Weihs *Scr. Mater.* **48** 1575 (2003)
108. A Duckham, S J Spey, J Wang, M E Reiss, T P Weihs, E Besnoin, O M Knio *J. Appl. Phys.* **96** 2336 (2004)
109. J Wang, E Besnoin, O M Knio, T P Weihs *Acta Mater.* **52** 5265 (2004)
110. WO/2007/0023489
111. J Wang, E Besnoin, O M Knio, T P Weihs *J. Appl. Phys.* **97** 114307 (2005)
112. A J Swiston Jr, E Besnoin, A Duckham, O M Knio, T P Weihs, T Hufnagel *Acta Mater.* **53** 3713 (2005)
113. Y Fu, H Du, W Huang, M Hu *Sens. Actuators, A* **112** 395 (2004)

[a] — *Dokl. Phys. Chem. (Engl. Transl.)*
[b] — *Appl. Phys. (Engl. Transl.)*
[c] — *Nonfer. Metall. Trans. (Engl. Transl.)*
[d] — *Bull. Russ. Acad. Sci., Phys. (Engl. Transl.)*
[e] — *Tech. Phys. (Engl. Transl.)*
[f] — *Phys. Solid. State (Engl. Transl.)*
[g] — *Russ. J. Phys. Chem. (Engl. Transl.)*
[h] — *Comb. Expos. Shoch Waves (Engl. Transl.)*
[i] — *J. Techn. Phys. Lett. (Engl. Transl.)*
[j] — *J. Exp. Theor. Phys. (Engl. Transl.)*
[k] — *Metallophys. New Technol. (Engl. Transl.)*